ELSEVIER

Journal of Structural Geology 26 (2004) 739–763

JOURNAL OF STRUCTURAL GEOLOGY

www.elsevier.com/locate/jsg

Boudinage classification: end-member boudin types and modified boudin structures☆

Ben D. Goscombe[a,*], Cees W. Passchier[b], Martin Hand[a]

[a]*Continental Evolution Research Group, Department of Geology and Geophysics, Adelaide University, Adelaide, S.A. 5005, Australia*
[b]*Institut fuer Geowissenschaften, Johannes Gutenberg Universitaet, Becherweg 21, Mainz, Germany*

Received 28 March 2002; received in revised form 25 August 2003; accepted 30 August 2003

Abstract

In monoclinic shear zones, there are only three ways a layer can be boudinaged, leading to three kinematic classes of boudinage. These are (1) symmetrically without slip on the inter-boudin surface (no-slip boudinage), and two classes with asymmetrical slip on the inter-boudin surface: slip being either (2) synthetic (S-slip boudinage) or (3) antithetic (A-slip boudinage) with respect to bulk shear sense. In S-slip boudinage, the boudins rotate antithetically, and in antithetic slip boudinage they rotate synthetically with respect to shear sense. We have investigated the geometry of 2100 natural boudins from a wide variety of geological contexts worldwide. Five end-member boudin block geometries that are easily distinguished in the field encompass the entire range of natural boudins. These five end-member boudin block geometries are characterized and named drawn, torn, domino, gash and shearband boudins. Groups of these are shown to operate almost exclusively by only one kinematic class; drawn and torn boudins extend by no-slip, domino and gash boudins form by A-slip and shearband boudins develop by S-slip boudinage. In addition to boudin block geometry, full classification must also consider boudin train obliquity with respect to the fabric attractor and material *layeredness* of the boudinaged rock mass. Modified or complex boudin structures fall into two categories: *sequential* boudins experienced a sequence of different boudin block geometry components during progressive boudinage (i.e. continued stretch), whereas *reworked* boudins were modified by subsequent deformational episodes (folded, sheared and shortened types). Correct classification of boudins and recognition of their modification are the crucial first stages of interpretation of natural boudin structures, necessary to employing them as indicators of shear sense, flow regime and/or extension axes in terranes otherwise devoid of stretching lineations.

Keywords: Boudin; Boudinage; Shear zones; Modified boudin; Kinematic indicator

1. Introduction

Boudinage is the disruption of layers, bodies or foliation planes within a rock mass in response to bulk extension along the enveloping surface. Boudin structures were first described by Ramsay (1881) and named by Lohest (1909). The huge variety that occur in nature have been the subject of considerable study (Wilson, 1961; Ramsay, 1967; Etchecopar, 1974, 1977; Hobbs et al., 1976; Lloyd and Ferguson, 1981; Lloyd et al., 1982; Blumenfeld, 1983; Simpson and Schmid, 1983; Hanmer, 1984, 1986; Van der Molen, 1985; Ramsay and Huber, 1987; Goldstein, 1988; Lacassin, 1988; DePaor et al., 1991; Hanmer and Passchier, 1991; Swanson, 1992, 1999). Nevertheless, there has been no attempt to erect a classification scheme for the full range of natural boudin structures. We propose a simple classification scheme that accounts for all simple unmodified boudin geometries that have been described and further, relate these end-member boudin geometries in a hierarchical scheme that considers their relationship to the three kinematic classes by which boudinage occurs (Table 1; Goscombe and Passchier, 2003). These kinematic classes are: (1) symmetrical boudins, which do not experience slip on the inter-boudin surface, forming by no-slip boudinage, and two asymmetrical classes with slip on the inter-boudin

☆ Extended datasets, Appendices B–C, can be found in the online version of this paper

* Corresponding author. Correspondence address: Geological Survey of Western Australia, P.O. Box 1664, Kalgoorlie, W.A. 6433, Australia.
E-mail address: ben.goscombe@doir.wa.gov.au (B.D. Goscombe).

0191-8141/$ - see front matter © 2003 Elsevier Ltd. All rights reserved.
doi:10.1016/j.jsg.2003.08.015

Table 1
Classification of boudinage of monoclinic symmetry

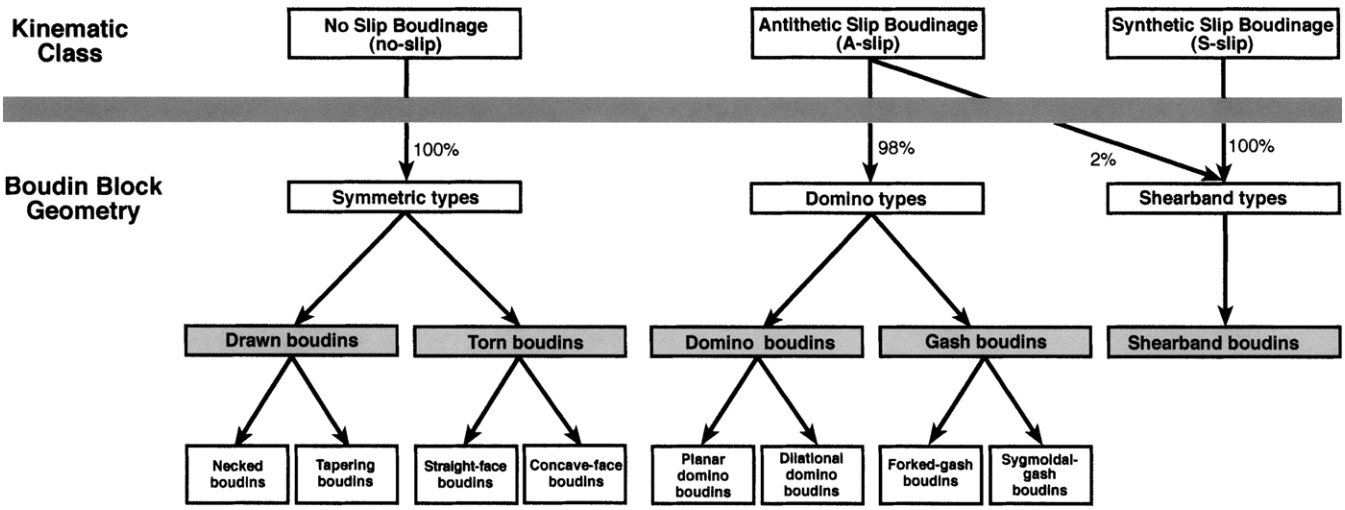

Below the thick shaded line are real boudin structures observable in rocks and above it, their correlating kinematic class of formation. Only boudin types that have not been modified are included here. All natural boudin structures can be classified in terms of the five end-member boudin block geometries that are highlighted by shading. These can be further sub-divided and the common examples are given (see also Fig. 3).

surface: (2) synthetic slip boudinage (S-slip) and (3) antithetic slip boudinage (A-slip) with respect to bulk shear sense.

In this paper, we classify natural boudin structures, both simple and modified, according to boudin block geometry, boudin train geometry and nature of the boudinaged material. This analysis is based on an extensive dataset, collected by the authors and collated from the literature, of quantitative data and qualitative features that describe boudin structures from a wide range of geological environments, spanning different flow regimes, rheological contrasts, metamorphic grade and strain. The boudin structures involved have been analysed in two integrated ways. First, natural groupings have been delineated based on boudin block geometries, boudin train geometries and the nature of the boudinaged material that can be recognized in the field. Second, we have related geometric groups to bulk flow and kinematic groups wherever possible. We largely restrict our study to boudin structures of monoclinic symmetry, considering the 2D-geometry in the profile plane normal to the long axis of the boudin. Where necessary, 3D effects are included. We use the results of this analysis to establish criteria that define simple end-member boudin types and subsequently recognize these components within complex modified boudin structures. The latter can be either: (1) reworked boudin structures modified by subsequent deformation unrelated to boudinage or (2) sequential boudin structures that contain multiple end-member boudin type components and formed by progressive boudinage.

2. The boudin dataset

Our dataset contains over 2100 boudins and collates the most important geometric parameters and features describing boudin structures illustrated in Fig. 1 and defined in Appendix A. A summary of the dataset is available in Table 2. Data were obtained primarily from the authors' field studies in a wide range of geological environments; including non-coaxial shear environments (Zambezi Belt in Zimbabwe; Ugab Terrane, Damara Orogen and Kaoko Belt in Namibia; and the Himalayas in Nepal), pure shear environments (Adelaidean Fold Belt in South Australia) and transtensional environments (oceanic crust on Macquarie Island). These data are augmented by measurement of photographs of boudins in true profile (normal to the boudin long axis) from the authors' collections and from the literature (Wilson, 1961; Ramsay, 1967; Weiss, 1972; Hobbs et al., 1976; Lloyd and Ferguson, 1981; Borradaile et al., 1982; Lloyd et al., 1982; Ramsay and Huber, 1983, 1987; Sengupta, 1983; Simpson and Schmid, 1983; Bosworth, 1984; Fry, 1984; Hanmer, 1984, 1986; Mullenax and Gray, 1984; Van der Molen, 1985; Davis, 1987; Goldstein, 1988; Malavielle and Lacassin, 1988; Hanmer, 1989; Laubach et al., 1989; Passchier et al., 1990; DePaor et al., 1991; Goscombe, 1991, 1992; Hanmer and Passchier, 1991; Swanson, 1992; Carreras and Druguet, 1994; Yamamoto, 1994; Daniel et al., 1996; Lisle, 1996; Conti and Funedda, 1998; Kraus and Williams, 1998; Roig et al., 1998). Data from photographs comprise 60% of the total dataset. The photographs do not permit the measurement of parameters

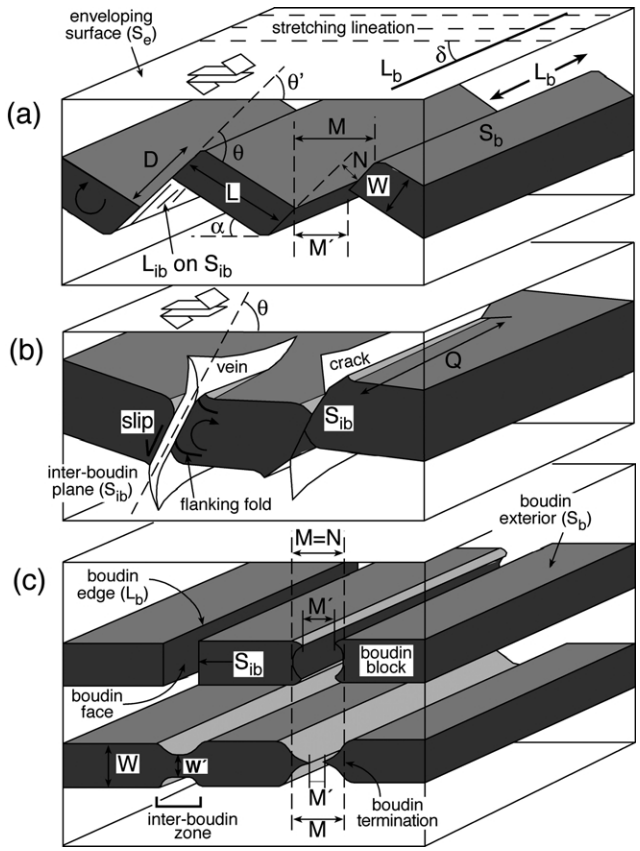

Fig. 1. Nomenclature and symbols of boudin structural elements and geometric parameters. (a) Asymmetric types (example is domino boudins). (b) Sigmoidal-gash boudin (left), forked-gash boudin (right). (c) Symmetric types; torn boudins (top) and drawn boudins (bottom). See Appendix A for full definitions. Layer in (b) is for reference only, typically gash boudins are in foliation boudinage. Shear sense is dextral in all cases.

out of the profile plane, such as those referenced to the boudin long axis, but all other important parameters can be measured.

All scales of boudinage are considered from metre-scale to mineral grain-scale (i.e. Simpson and Schmid, 1983; Lister and Snoke, 1984; Simpson, 1984; Goscombe, 1991, 1992; Yamamoto, 1994; Goscombe and Everard, 2000; Goscombe, unpublished data). It was found that nearly all groups of boudins, with their characteristic parameters, are developed on both the mesoscopic and the mineral grain-scale. Parameters measured from both outcrop and photographs of the same structure indicate that there is no systematic skewing of the data with either measurement source. Consequently, data from photographs (i.e. from the literature) are considered equally accurate as those measured in the field. Absolute errors on measurements can only be estimated, but comparison between outcrop and photographic data offer limits. The average absolute difference between measurements from outcrop and photograph of the same structure is on the order of $\pm 4.5°$ for angular parameters and $\pm 5–10\%$ for linear parameters.

3. Boudin structural elements

3.1. General parameters

Boudins are complex and highly variable 3D structures and so to be uniquely described requires a large number of quantifiable dimensional and angular parameters relating the structural elements (Fig. 1; Appendix A). No consistent nomenclature for boudin structural elements or geometric parameters has been adopted in the literature, even for the simplest system of symmetric boudinage (Jones, 1959; Wilson, 1961; Hobbs et al., 1976; Penge, 1976; Lloyd et al., 1982). Thus, a suite of nomenclature for structural elements and geometric parameters that uniquely describes all possible boudin structures is adopted in this study (Fig. 1) and defined in detail in Appendix A.

A description of the nature of boudinage involves first of all the overall nature of the boudinaged element. The nature or degree of *layeredness* of the boudinaged material forms a continuous spectrum that can be classified into the following. (1) Object boudinage of a competent object of limited dimensional extent such as a mineral grain. (2) Single-layer boudinage of a competent layer in a less competent host (Ghosh and Sengupta, 1999). (3) Multiple-layer boudinage of a packet of thin competent layers (Ghosh and Sengupta, 1999). A variation is ‘composite boudins’ composed of boudinaged sub-layers within a boudinaged packet of layers, giving nested boudins of different scale (Ghosh and Sengupta, 1999). (4) Foliation boudinage (Lacassin, 1988; Mandal and Karmakar, 1989; Ghosh and Sengupta, 1999) of a foliated rock devoid of, or irrespective of, layers of differing competence (Fig. 2). An alternative way of describing this class is in the ratio *C*/*G* of the width of more competent or boudinaged units against the grain-size; if this ratio is less than 10, boudinage does not occur in distinct layers and is known as foliation boudinage.

Boudinage is the disruption of layers, bodies or foliation planes within a rock mass resulting in boudin blocks (simply called boudins). For single-layer boudinage, it is easy to define a boudin exterior (S_b), the disrupted fragments of the original bounding surfaces of the boudinaged body. For multiple-layer and foliation boudinage, S_b can be defined as the surface connecting the boudin edges or tips of boudin faces (Fig. 1). In addition, an enveloping surface (S_e) can usually be defined for a train of boudins (Fig. 1). S_e is commonly, but not always, parallel to the penetrative foliation (S_p) in the host rock to the boudins. The orientation of the boudin long axis, boudin edge or neck zone can be described as a linear feature, L_b (Fig. 1). L_b is by definition normal to the extension axis (L_e) of the boudin structure (Appendix A). An angle δ can be defined between L_b and the dominant stretching lineation (L_p) in the host rock to the boudins. This angle δ is usually orthogonal, in which case boudins and adjacent structures have a monoclinic 3D geometry. The vast majority of boudins investigated have monoclinic symmetry and in such cases parameters

Table 2
Mean values of parameters and diagnostic features of the five end-member boudin block geometries in foliation-parallel boudin trains. Drawn boudins have been further sub-divided into necked and tapering boudins

	Asymmetric boudins			Symmetric boudins		
	Domino boudins	Gash boudins	Shearband boudins	Torn boudins	Tapering boudins	Necked boudins
Number of boudins	479	79	340	499	361	94
Boudin shape and nature						
Inter-boudin surface (S_{ib})	Sharp, straight	Sharp, sigmoidal or forked	Ductile, sigmoidal/straight	Sharp, straight or concave	None	None
S_{ib}–S_e relationship	S_{ib} terminates as S_e	S_{ib} discordant to S_e	S_{ib} terminates as S_e	S_{ib} discordant to S_e	No S_{ib}, stretch of S_e	No S_{ib}, stretch of S_e
Boudin shape	Angular rhomb	Angular rhomb	Sigma lens or rhomb	Angular block	Convex lens	Pinch and swell
Associated kinkbands	None	None	Rare	None	None	None
Inter-boudin zone fill	Host (68%), vein (32%)	Vein (75%), host (25%)	Host (96%), vein (4%)	Vein (74%), host (26%)	Host (95%), vein (5%)	Host (99%), vein (1%)
Foliation boudinage	35%	95%	0%	8%	0%	0%
Typical boudinaged layer[a]	Psammite, calc-silicate	Psammite	Quartz-vein in schists	Calc-silicate, psammite	Mafic, aplite	Aplite
Preferred metamorphic grade[a]	Low-grade	Low-grade	High-grade	Low-grade	High-grade	High-grade
Boudinage with respect to tectonic transport						
Slip on S_{ib}	A-slip (98%)	A-slip (68%), no-slip (30%)	S-slip (100%)	None (99%)	None (100%)	None (100%)
Block rotation sense	Synthetic (98%)	Synthetic (64%), none (32%)	Antithetic (100%)	None (97%)	None (100%)	None (100%)
Kinematic class	A-slip (98%)	A-slip (100%)	S-slip (100%)	No-slip (96%)	No-slip (94%)	No-slip (100%)
Atypical geometry for kinematics	3%	0%	0%	NA	NA	NA
Flanking fold on S_{ib}	42%	62%	0%	NA	NA	NA
Synthetic drag on S_{ib}	13%	0%	98%	NA	NA	NA
No deflection on S_{ib}	45%	38%	2%	100%	NA	NA
Vergence by S_{ib} inclination	Forward vergent (100%)	forward Vergent (91%)	Backward vergent (100%)	Forward vergent (56%)	NA	NA
Second episode of boudinage[b]	10%	5%	11%	8%	35%	8%
Angular parameters (mean)						
α—relative block rotation	18°	10°	16°	None	None	None
θ—block shape	72°	81°	39°	85°	NA	NA
θ'—inclination of S_{ib} wrt S_e	54°	70°	24°	85°	NA	NA
δ—L_b wrt $L_{stretching}$[b]	71°	73°	77°	71°	74°	71°
Distribution of L_b wrt $L_{stretching}$[b]	Symmetrical around $L_{stretching}$	86% clockwise of $L_{stretching}$	Symmetrical around $L_{stretching}$	Symmetrical around $L_{stretching}$	Symmetrical around $L_{stretching}$	63% clockwise of $L_{stretching}$
Dimensional parameters (mean)						
L/*W*—aspect ratio	1.99	1.83	3.57	2.90	4.07	2.59
D/*W*—normalized displacement	0.49	0.12	2.20	0.00	NA	NA
% with displacement on S_{ib}	100%	85%	100%	4%	NA	NA
N/*L*—S_{ib} dilation (if present)	0.17	0.05	0.02	0.41	NA	NA
% with dilation across S_{ib}	29%	78%	2%	100%	NA	NA
M/*L*—normalized extension	0.32	0.07	0.66	0.41	0.77	0.29
Stretch—extension of S_e	126%	104%	160%	141%	177%	129%
% with isolated boudins	17%	0%	70%	<98%	93%	0%
Flanking fold half wavelength/*W*	0.65	0.31	1.21	0.14	NA	NA

Data sourced from all investigation areas and literature. Symbols and nomenclature defined in Appendix A.

[a] Normalized for both the total number of readings of each boudin block geometry category and total number in each rock-type or metamorphic grade category.

[b] Data from Kaoko Belt only. Brackets indicate proportion of data in the indicated category.

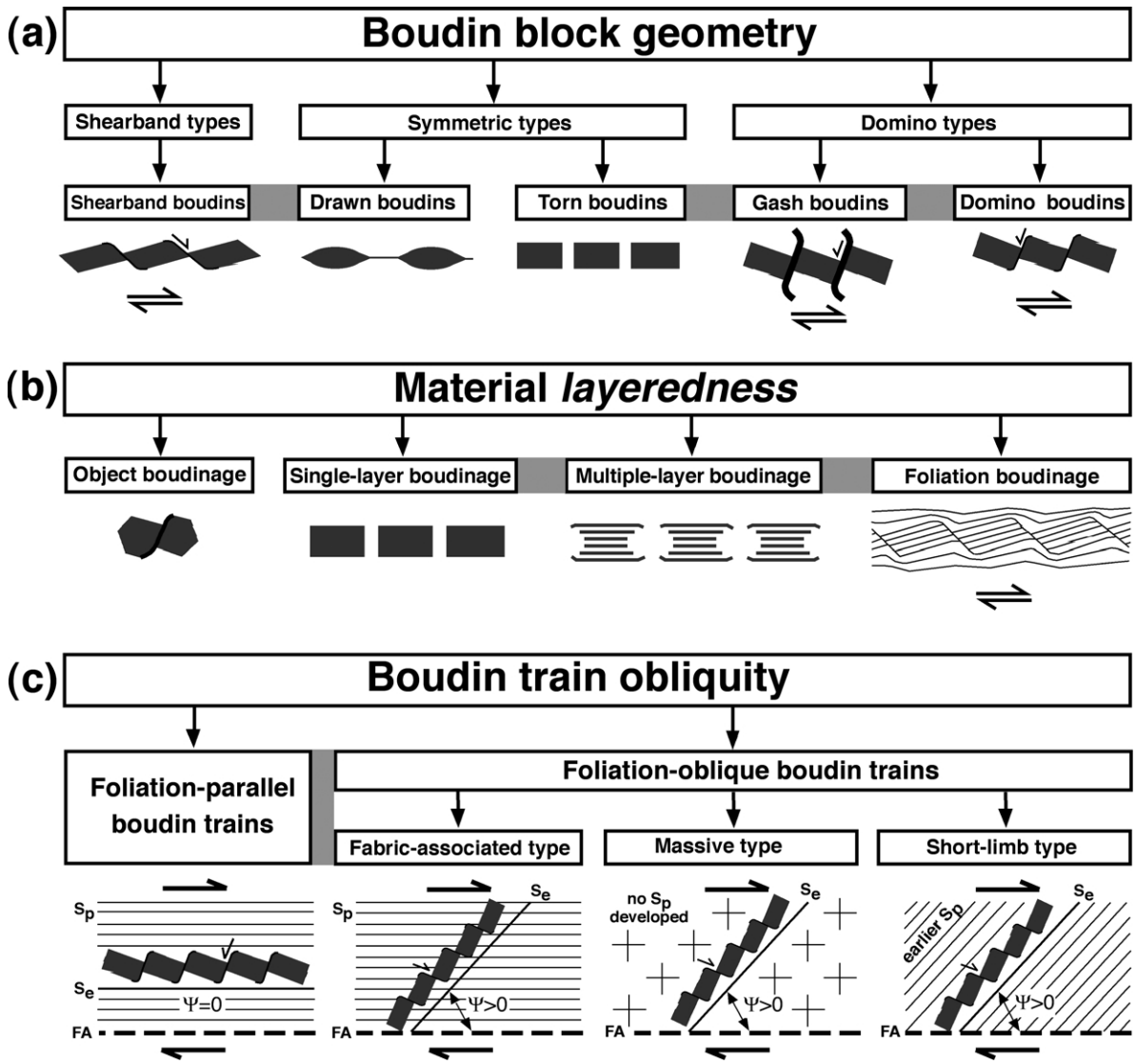

Fig. 2. Full classification scheme, outlining the three aspects that describe the full geometry of any boudin train. Diagrams illustrate a representative example from each type. Shading indicates where transitions exist between groups. All diagrammatic examples illustrating boudin train obliquity have domino boudin block geometry and the fabric attractor (FA) is assumed for simplicity to be parallel to the pervasive foliation (S_p) where present. Note: the foliation-parallel boudin train formed by A-slip boudinage and all foliation-oblique boudin train examples formed by S-slip boudinage (cf. Goscombe and Passchier, 2003). Shear sense is dextral in all cases.

measured in the profile plane normal to L_b are sufficient to fully describe boudin geometry. In some cases, however, $\delta < 90°$ and the 3D geometry of the boudins and adjacent host rock is triclinic. A full 3D-description of the structure is necessary in such cases.

In all cases, boudin blocks are separated by either a discrete surface called the boudin face, or an extensional gap known as the inter-boudin zone or neck zone (Fig. 1). The inter-boudin zone is a complex feature into which there is material transfer by host inflow, vein infill or combinations of both (Fig. 3). Host inflow is typically ductile, resulting in deflection of the enveloping surface and formation of half folds ('scar folds', Hobbs et al., 1976), with characteristic peaked and cuspate shapes that are best known in their association with boudin structures. The less common scenario of brittle host inflow is accommodated by a network of minor faults in the inter-boudin zone, aligned at a high angle to layering. True dilation and vein infill is typically hydrothermal material (such as quartz, micas and carbonate) at lower amphibolite facies and lower grade conditions and pegmatite and partial melt material at upper amphibolite and granulite facies.

For any boudin type with boudin faces or inter-boudin zones, an inter-boudin surface (S_{ib}) can be defined. In asymmetric boudin structures without dilation, S_{ib} is an inclined, discrete surface that coincides with the boudin face, along which boudins were laterally displaced and which arcs into parallelism with the enveloping surface (S_e) at the boudin edge (Figs. 1 and 4). In symmetric and asymmetric boudins with dilation, S_{ib} is not a discrete

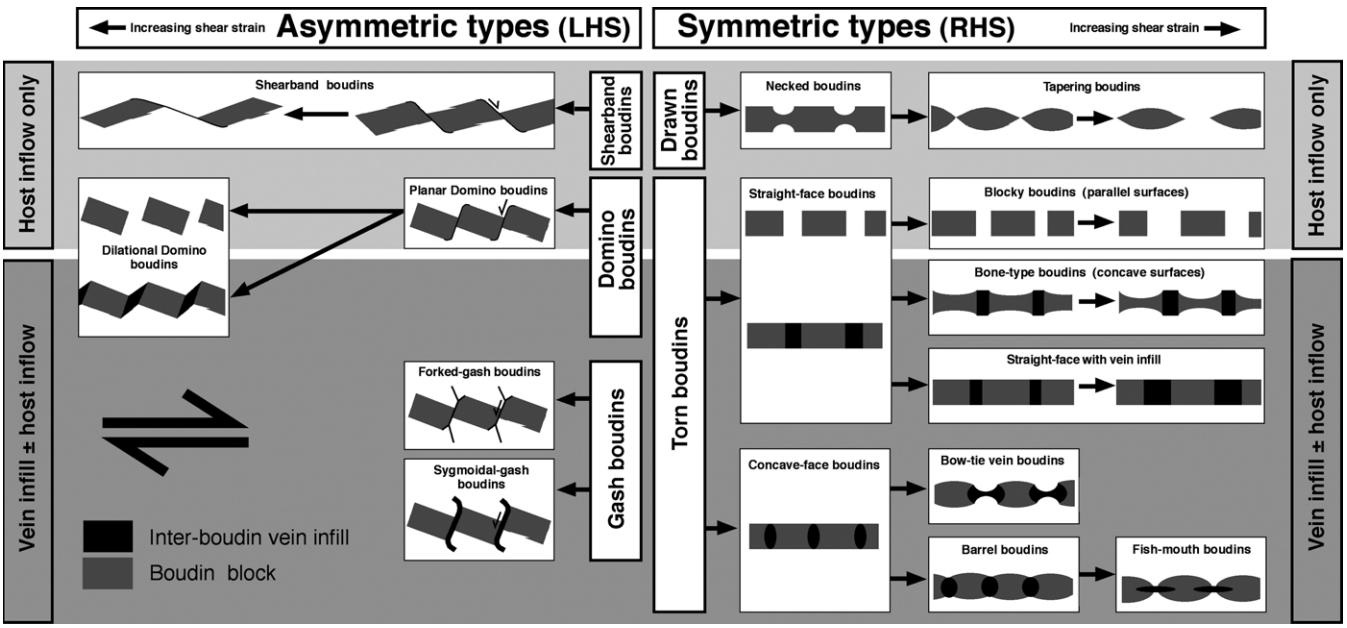

Fig. 3. Schematic drawings of variations in the five end-member boudin block geometries (in centre of diagram) and relationship to both shear strain (outwards from centre of page) and relative proportion of host inflow (i.e. scar folds) versus vein infill in the inter-boudin zone (down page). An increasing ratio of host inflow over vein infill indicates increasing flattening strain associated with layer extension. Asymmetric (LHS) versus symmetric (RHS) grouping of boudin type illustrates that shearband types are essentially asymmetric drawn boudins and domino types are essentially asymmetric torn boudins. Shear sense is dextral in all asymmetric cases, as shown.

surface developed in the rock but is the imaginary 'skeletal' median plane in the inter-boudin zone (Fig. 1b). In blocky torn boudins this is typically sub-parallel to the boudin face (Fig. 1c). In drawn boudins no S_{ib} as defined above is developed, thus an arbitrary 'S_{ib}' defined as the median plane connecting boudin terminations is used in these cases (Fig. 4c; Appendix A). In contrast to faults or shear zones, the S_{ib} is confined to the boudinaged layer and so differs from 'pseudo-boudinage' or 'structural slicing' (Bosworth, 1984), where layer disruption is due to penetrative faults and shear zones that extend beyond the disrupted layer.

3.2. Parameters quantifying boudin block geometry

In order to compare boudins, quantitative parameters must be defined that capture the essential features of these structures (Fig. 1; Appendix A). It is not always necessary to describe the geometry of boudins with great accuracy, and in that case, a few essential and most diagnostic parameters, such as those listed in Table 2, are sufficient for quantitative characterization. For a complete description of skeletal boudin geometry in a section normal to L_b, the following parameters suffice (Fig. 1): L, the length of individual boudin blocks; W, boudin thickness or width; θ, the angle between S_b and S_{ib}; D, the displacement of S_b along S_{ib}; and N, the width of the inter-boudin gap measured normal to S_{ib}.

Some additional parameters can be useful in describing boudin structures, although they are dependent on the five basic elements mentioned above. These additional parameters are: the inclination of S_{ib} (θ'), the relative block rotation (α; the extension of the enveloping surface (stretch); boudin block isolation (M') and layer extension (M). These latter parameters are related to the basic ones by the equations:

$$\alpha = S_b \wedge S_e = \arctan(D\sin\theta(L + D\cos\theta)) \quad (1)$$

$$\theta' = S_e \wedge S_{ib} = \theta - \alpha \quad (2)$$

$$M = D\cos\theta' + N(\cos\alpha\sin\theta) \quad (3)$$

$$M' = M - W(\cos\theta'\cos(90^\circ - \theta)) \quad (4)$$

$$\text{stretch} = (M + L\cos\alpha)/L \quad (5)$$

Boudinage ranges in scale from mineral grain- to metre-scale and thus absolute dimensional parameters are of little interest in defining boudin geometry. Consequently, all dimensional parameters, such as displacement on S_{ib} (D), dilation across S_{ib} (N), boudin isolation (M') and layer extension (M), are normalized with respect to width (W) or length (L) of the boudin block as outlined in Table 2. The angle θ and three independent normalized parameters suffice to completely describe skeletal boudin geometry.

Boudin block shape is given as a description of the outer surface of the boudin in profile. This is typically characterized by groupings with descriptive names that encompass a circumscribed range in values of quantitative and qualitative parameters. The most important parameters are aspect ratio (L/W), shape of the boudin face, shape of the boudin exterior and degree of asymmetry (θ) (Figs. 1 and 4). Shape of the boudin face in profile ranges from terminating at a point (tapering or lenticular boudins), convex-face (such as 'sausage' boudins), straight-face (such as blocky boudins), concave to extremely concave and folded against

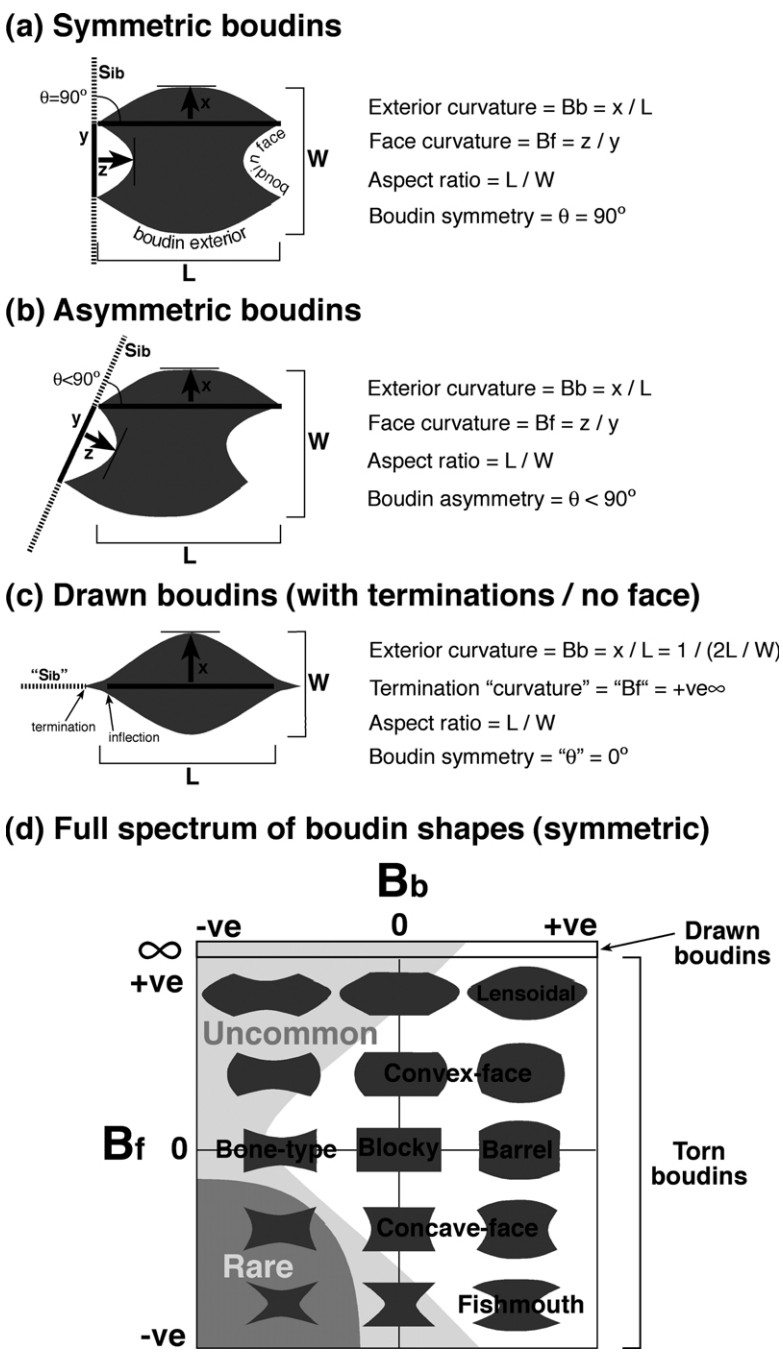

Fig. 4. (a)–(c) Definition of the four parameters that comprehensively define boudin block shape. θ = Symmetry of boudin block, L/W = aspect ratio, B_b = curvature of boudin exterior and B_f = curvature of boudin face. (d) Range of symmetric boudin block shapes and nomenclature of the most common examples.

itself as in the case of 'fishmouth' or 'false-isocline' boudins (Figs. 3 and 4). Shape of the boudin exterior (S_b) can be concave (such as 'bone-type' boudins), convex (such as 'barrel' boudins) or parallel to each other (parallelograms such as blocky boudins; Figs. 3 and 4). Boudin exteriors may be parallel but not planar only in cases of reworked boudin structures that have been sheared or folded (described later). Boudin block asymmetry is defined by the angle between S_{ib} and S_b (θ), ranging from symmetric boudins with high θ (such as blocky boudins) through rhomb shapes to asymmetric tapering shapes with low θ. Degree of angularity of the boudin edge may be angular such as blocky boudins or curved such as sausage, sigma-shaped and lenticular lenses.

In some cases, a more precise geometric description of boudin blocks is needed. Boudin shape can be simply quantified by ratios that define the degree of convex or concave curvature of the boudin faces and boudin exteriors (Fig. 4; Appendix A). The ratio describing the curve of the boudin exterior (B_b) is defined by the maximum normal

deviation of the boudin exterior out from (+ve) or into the boudin interior (− ve), from the straight line connecting the boudin edges, divided by the length of this line (i.e. L). In the same way, the curve of the boudin face (B_f) is defined by the maximum normal deviation of the boudin face out from (+ve) or into the boudin interior (− ve), from the straight line connecting the edges of the boudin face, divided by the length of this line (Fig. 4). For asymmetric boudins, the same can be applied, and the combination of L/W and θ, B_b and B_f is in most cases sufficient to describe the shape of boudin blocks for practical purposes (Fig. 4).

4. Boudinage asymmetry

Many boudins are asymmetric and are potential shear sense indicators (Goscombe and Passchier, 2003). Several parameters define the asymmetry vergence of sets of boudin blocks in a boudin train, as follows:

1. The direction of inclination of S_{ib} defined by the angle (θ) between S_{ib} and S_b is either in the opposite direction to shear sense and named forward-vergent or inclined in the same direction as shear sense and named backward-vergent. Swanson (1992, 1999) used the terms 'forward-tilted' or 'forward-rotated' and 'backward-tilted' or 'backward-rotated' to indicate vergence by the direction of hypothetical tilting of an originally orthogonal S_{ib} with respect to shear sense. The S_{ib} did not necessarily rotate into the inclined orientation (Goscombe and Passchier, 2003) and so the terms 'tilting' and 'rotated' are misleading and should be discontinued.
2. Lateral displacement of the boudin exterior (S_b) on the S_{ib}, also known as slip on the inter-boudin surface, is expressed by a value D. Its sense can be either synthetic (S-slip) or antithetic (A-slip) with respect to bulk shear sense (Figs. 2 and 3). Directly associated with this slip is the direction of relative rotation (α) of S_b with respect to the enveloping surface, S_e (block rotation). In S-slip boudinage, block rotation is antithetic and in A-slip boudinage, block rotation is synthetic with respect to bulk shear sense.
3. Foliation or layering within the boudin may be deflected in a narrow zone parallel to S_{ib}; this can be in the same (synthetic drag) or opposite (antithetic drag) direction as the displacement sense on S_{ib} (Fig. 5b and c). Such behaviour has been described as 'flanking structures' by Passchier (2001). Structures with synthetic drag are known as flanking shear bands and those with antithetic drag as flanking folds (Grasemann and Stuwe, 2001; Passchier, 2001). Flanking folds on S_{ib} contribute an additional component of block rotation that is synthetic with whole block rotation (Figs. 5b and 6). Flanking folds on S_{ib} are not to be confused with the flanking folds that formed by a similar mechanism, but on a different scale and different site, on the margin of the trace of foliation-oblique boudin trains (Fig. 5a; Hanmer and Passchier, 1991; Ramsay and Lisle, 2000).
4. The sigmoidal trace of S_{ib} has S- or Z-shape defining a spiral vergence that is either synthetic or antithetic to bulk shear sense (Fig. 1b). This vergence is analogous to that in sigmoidal tension gashes.

Comparison of natural boudin geometry and bulk shear sense indicate that the characteristic geometry of different end-member asymmetric boudin types can indeed be linked to bulk shear sense and thus kinematic class of boudinage in many cases, as explained in detail in Goscombe and Passchier (2003). Here, we focus on boudinage classification, which includes but is not restricted to the record of kinematics.

5. End-member boudin block geometry types

Boudins in our dataset can be rationalized into a minimal set of five distinct end-member boudin block geometries, which can be readily recognized in the field (Table 1; Figs. 2 and 3). These are domino, shearband, gash, drawn and torn boudins. These can be grouped into symmetric types (drawn and torn boudins) and two asymmetric boudin groups: domino types (domino and gash boudins) and shearband types (Table 1). The five end-member boudin block geometries are characterized in detail below, geometric parameter fields are presented in Figs. 6–8, diagnostic features and average parameters are summarized in Table 2, typical forms are represented in Figs. 1–3 and natural examples in Fig. 9. The essential elements required to define all boudin types are presented here; further details for asymmetric boudins are provided by Goscombe and Passchier (2003).

5.1. Domino boudins

Domino boudin blocks are asymmetric, usually short, stubby rhomb shapes with angular edges. In most cases S_{ib} is a discrete sharp surface (planar domino boudins) or in 29% of investigated cases is a set of parallel terminal faces either side of an inter-boudin zone filled with vein material or host rock (dilational domino boudins; Fig. 9a; Table 1). Dilational domino boudins have straight S_{ib}; those with sigmoidal S_{ib} trace are classified as gash boudins (Table 1). S_{ib} is at a high angle to S_b (θ typically 55–90°; Fig. 7) and together with typically low lateral displacement (D) along S_{ib}, implies low extension of the enveloping surface (stretch averages only 126%; Table 2). In all domino boudins, inclination of S_{ib} is in the opposite direction to bulk shear sense, defining forward-vergent structures, and almost all correspond to A-slip boudinage (Table 1). Apparent 'drag' on S_{ib}, where present, is antithetic to slip on S_{ib}, resulting in development of

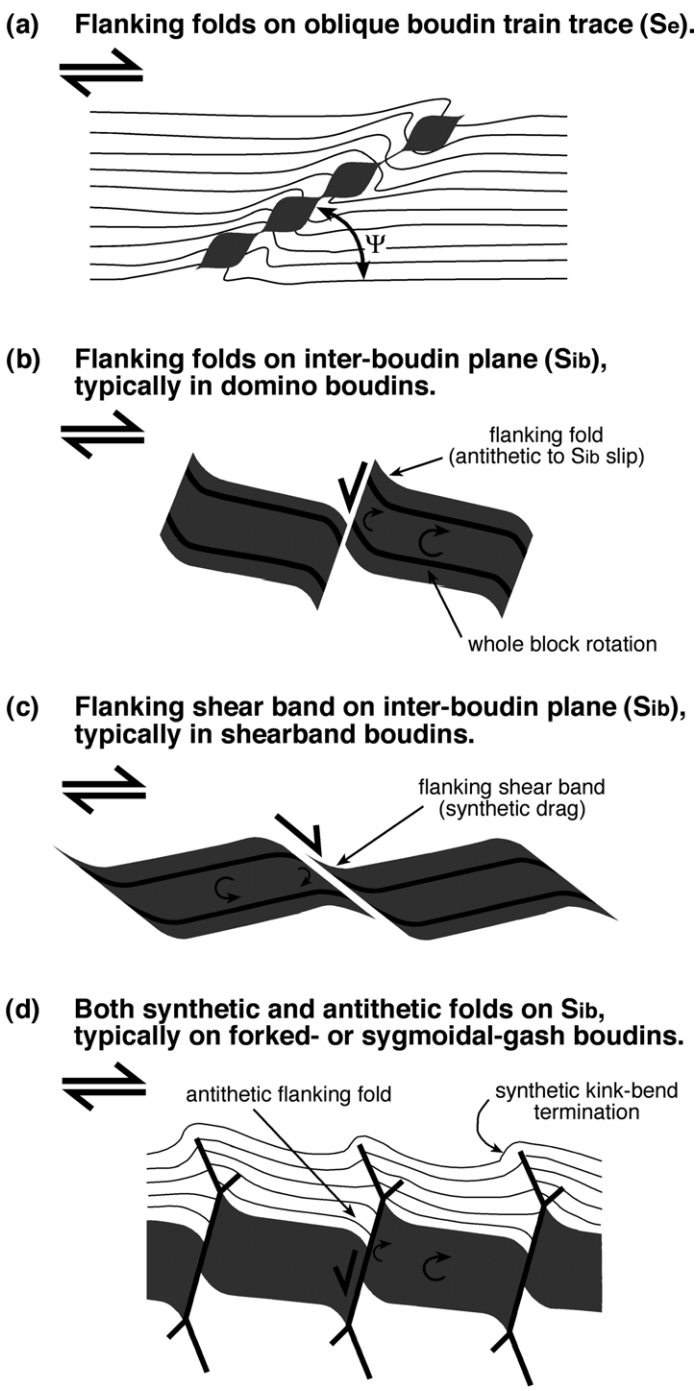

Fig. 5. Types of flanking structures associated with boudins: nomenclature after Passchier (2001). (a) Flanking folds on the margins of foliation-oblique boudin trains. (b) Flanking folds (antithetic 'drag') on the boudin face (S_{ib}) of domino boudins. (c) Flanking shear-band (synthetic 'drag') on the boudin face of shearband boudins. (d) Combination of synthetic 'drag' (kink-bend termination) and antithetic 'drag' (flanking fold) on the boudin face of gash boudins.

flanking folds (Hudleston, 1989; Passchier, 2001; Figs. 1b and 5). Antithetic flanking folds on S_{ib} are diagnostic of domino-type boudins, including gash boudins, with high *L*/*W* ratio, and do not occur in other boudin types or domino boudins with low aspect ratios (Fig. 6).

Domino boudins of the geometry described above have been variously called: 'tuilage/tiling structures' (Blumenfeld, 1983; Hanmer and Passchier, 1991), 'book shelf sliding' (Ramsay and Huber, 1987), 'sheared stack of cards model' (Etchecopar, 1974, 1977; Simpson and Schmid, 1983), 'type I asymmetric pull aparts' (Hanmer, 1986), 'turf' or 'asymmetric blocky boudins' (Hanmer, 1984) and 'extensional fracture boudinage' or 'forward-rotating orthogonal vein geometry' (Swanson, 1992, 1999). The term domino has been used informally by many workers (i.e. Hanmer and Passchier, 1991), is widely understood and

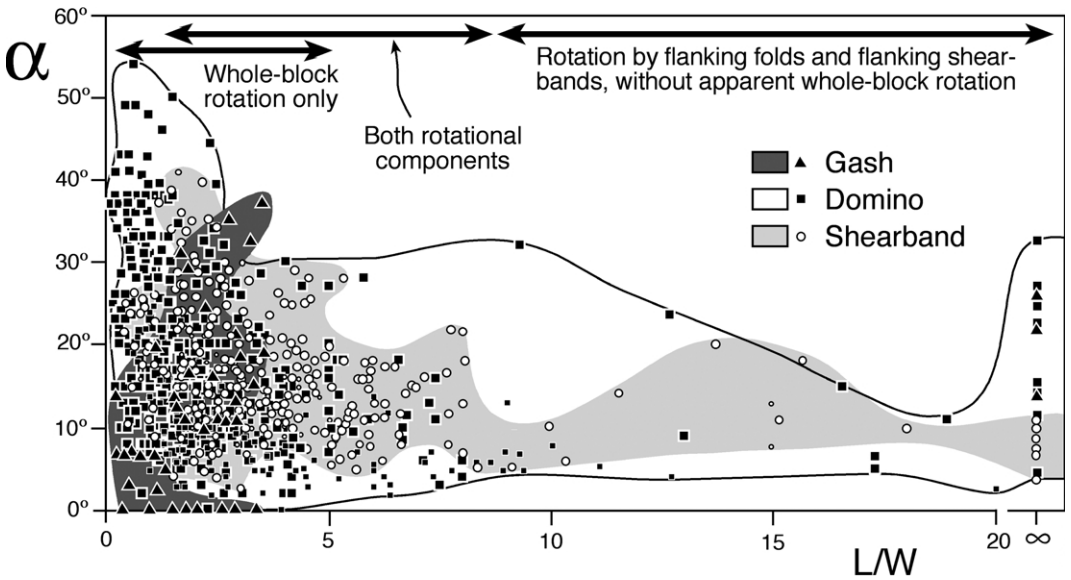

Fig. 6. Relationship between relative block rotation (α) and aspect ratio (L/W), by boudin block geometry type. Range of the two types of block rotation—whole-block rotation and rotation in the boudin face zone by flanking folds—are indicated with respect to L/W.

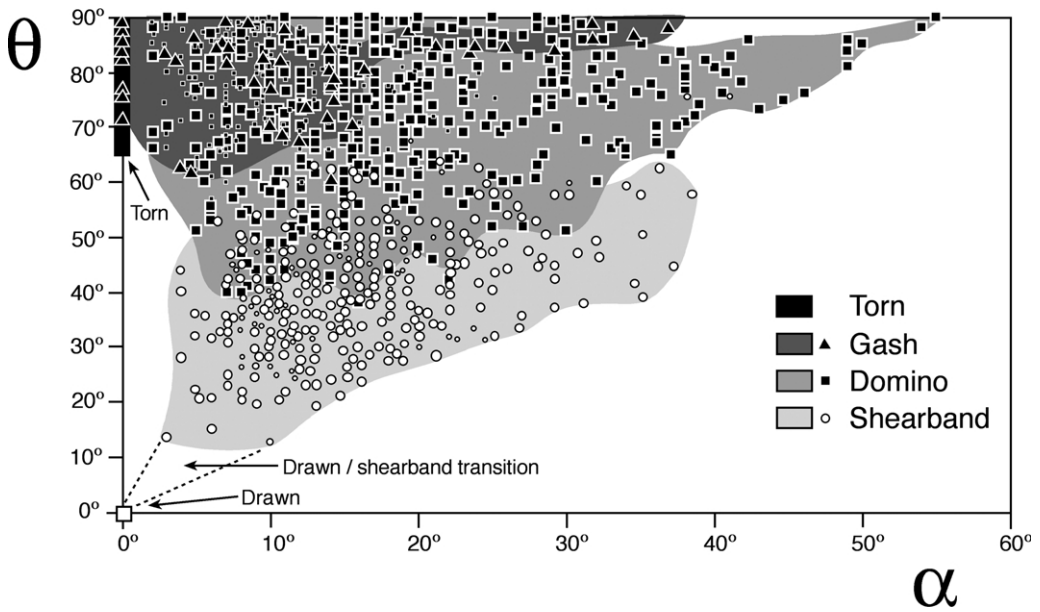

Fig. 7. Relationship between boudin block shape (θ) and relative block rotation (α) for each boudin block geometry type. Large symbols represent foliation-parallel boudin trains and small symbols represent foliation-oblique boudin trains.

best encapsulates their geometry in one word and so has been adopted for this classification of boudins.

5.2. Gash boudins

Some domino-type boudins that formed almost exclusively by foliation boudinage have such a distinct set of characteristics that they can be grouped separately from domino boudins (cf. Goscombe and Passchier, 2003). All are dilational and have a sigmoidal S_{ib} trace that is either a smooth continuous curve or of angular geometry (Fig. 1b); thus we have named these gash boudins (Table 1). Smooth forms resemble sigmoidal tension gashes (Fig. 1b). Angular forms are more complex, and typically comprise a straight

Fig. 8. Relationship between dimensional ratios, with fields for each boudin block geometry type outlined. (a) Normalized displacement on S_{ib} (D/W) versus boudin aspect ratio (L/W). (b) Relative thickness of either the layer (drawn boudins) or vein infill (torn boudins) in the inter-boudin zone relative to the boudin. (c) Normalized dilation across S_{ib} (N/L) versus normalized layer extension (M/L). Not all drawn boudins have been represented, because in all cases $N/L = 0$ and the distribution is similar to that of shearband boudins.

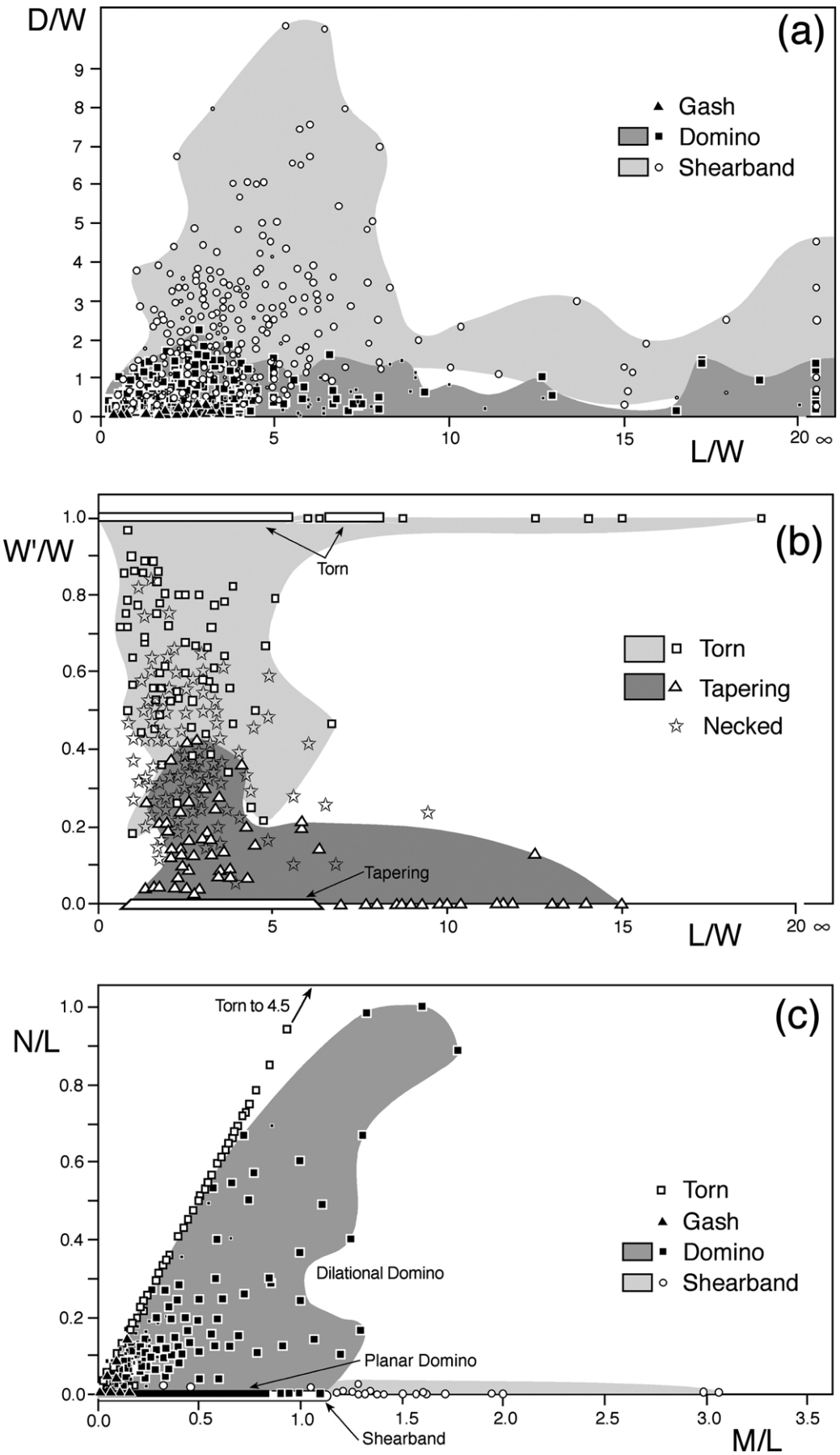
D/W
(a)
Gash
Domino
Shearband
L/W
W'/W
(b)
Torn
Tapering
Necked
L/W
N/L
(c)
Torn to 4.5
Dilational Domino
Planar Domino
Shearband
Torn
Gash
Domino
Shearband
M/L

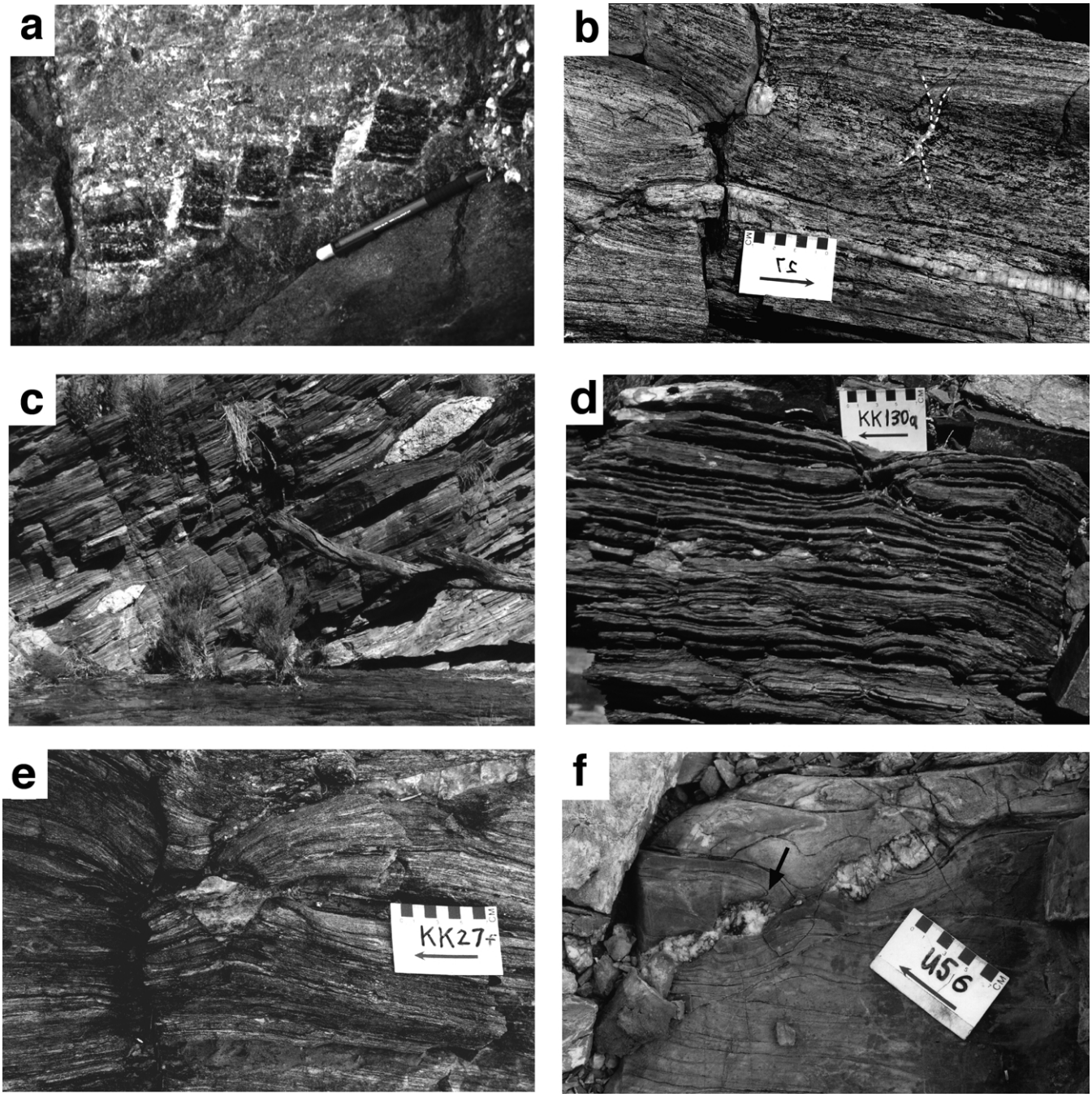

Fig. 9. Examples of typical unmodified end-member boudin block geometries. (a) Dilational domino boudins in carbonate from Nanga Parbat Massif in Pakistan. (b) Forked-gash boudin in sheared feldspathic quartzite from Kaoko Belt, Namibia. (c) Tapering boudins of pegmatite in amphibolite-grade gneisses from Huckitta Creek, Arunta Block. (d) Multiple-layer boudinage of inter-layered quartzite and carbonate, with drawn boudin geometries, from the Kaoko Belt in Namibia. (e) Foliation boudinage of sheared quartzo-feldspathic gneisses from the Kaoko Belt, Namibia. Torn boudins with extreme concave face, commonly called fishmouth boudins. (f) Foliation-oblique boudin train of tapering boudins of discordant quartz vein in carbonate matrix, Ugab Zone, Namibia. Note flanking fold (arrow) on the margin of the boudin train, due to rotation of the train to lower angles (Ψ) with the pervasive foliation, during progressive deformation. Bulk shear sense is dextral in all asymmetric cases (some images have been flipped about a vertical axis to facilitate comparison).

central section and forked or inclined crack terminations (Figs. 1b and 9b), which have been described by Swanson (1992) as 'swordtail' and 'fishmouth' terminations. Swanson (1992) called the two gash boudin types 'sigmoidal boudin partings' and 'reoriented extension fractures', respectively. We favour sigmoidal-gash boudins and forked-gash boudins as names for these geometries.

Gash boudins have some other special characteristics. The central portion of S_{ib} is nearly orthogonal (θ averages 81°) to the boudin exterior (S_b). Aspect ratios of boudin

blocks are extremely low (Table 2) and unlike all other boudin types, the extent (Q; Fig. 1b) of the boudin structure along L_b is clearly finite, averaging only 90% of the boudin length, L. Dilation and associated vein infill are common but narrow (Fig. 8c) and displacement is low (Fig. 8a), resulting in very low extension of the enveloping surface (stretch averaging only 104%). Slip on S_{ib} is usually antithetic to bulk shear sense and S_{ib} inclination is forward-vergent (Table 2). Flanking folds are common in the central portion of S_{ib} and synthetic drag is only evident at the tips of S_{ib} (Fig. 5d), resulting in the 'kink-bend' terminations described by Swanson (1992) and Grasemann and Stuwe (2001). Spiral vergence defined by the sigmoidal trace of S_{ib} is synthetic to bulk shear sense.

5.3. Shearband boudins

Shearband boudins are asymmetric with rounded rhomb to tapering lens shapes, typically with relatively high aspect ratios (Fig. 8a). The obtuse edge of the boudin is often rounded and the acute edge is drawn into a tapering wing by drag on S_{ib}. Dilation across S_{ib} and associated vein infill almost never occurs (Fig. 8c). S_{ib} is typically a thin ductile shear zone with associated ductile grain refinement and grain-shape fabric. In some cases, S_{ib} constitutes a wider ductile zone displacing adjacent boudins with the appearance of asymmetric drawn boudins. S_{ib} is straight to curviplanar and at a low angle to S_b, with θ typically less than 60° (Fig. 7). Lateral displacement on S_{ib} is the highest of all boudin types (Fig. 8a). Consequently, extension of S_e is high (Fig. 8c), with stretch averaging 160% and commonly (69% of investigated cases) results in complete isolation of adjacent boudin blocks (Table 2). All shearband boudins form by S-slip boudinage (Table 1) and are backward-vergent. Drag on S_{ib} is almost always evident and synthetic to slip (Table 2)—a diagnostic feature that is responsible for the tapering sigma shapes of the boudin blocks.

Shearband boudins of foliation boudinage type are probably more common than represented in our dataset. Such structures would be expressed as sigma-shaped lenses of schist within schist host, best described as 'foliation fish' (Hanmer, 1986) and akin to mica fish (Lister and Snoke, 1984), forming a continuum between what is true boudinage and what is due to a penetrative C or C′ shear-band cleavage. The geometry of 'pseudo-boudinage' structures formed by penetrative C′ shear-band cleavages has been investigated ($n = 15$), and these differ in no way from shearband boudins except for the lateral extent of the C′-surface (equivalent to S_{ib}). Mineral grain-scale shearband boudins do occur; mica fish (Lister and Snoke, 1984) may be a common example with forms that mimic the typical sigma shape of mesoscopic shearband boudins.

Shearband boudins of the geometry described above have been called 'asymmetric pinch-and-swell structures' (Hanmer, 1984, 1986; Hanmer and Passchier, 1991), drawing attention to the continuum between symmetric drawn boudins and asymmetric shearband boudins (Fig. 2a). In addition, shearband boudins have been variously named 'type II asymmetric boudins' (Goldstein, 1988), 'sigmoidal boudinage' (Ramsay, 1967), 'shear-fracture boudinage' (Swanson, 1992), 'backward-rotated shear-band boudins' (Swanson, 1999), 'surf asymmetric pull-apart structures' (Hanmer, 1984), 'asymmetric extensional structures' (Lacassin, 1988) and 'asymmetric pull-apart structures': type 2A without discrete S_{ib} and type 2B with discrete S_{ib} (Hanmer, 1986). We have adopted the name shearband boudins because their geometry so closely resembles that of shear-band cleavages (Simpson, 1984; Lister and Snoke, 1984) and in a single word best invokes an image of their form.

5.4. Drawn boudins

Both shearband and domino boudins grade into symmetric boudin structures. These symmetric boudins can be grouped into those that experienced apparent 'ductile' stretch of the layer (named drawn boudins) and those where the layer was dissected by high-angle, sharp, apparently 'brittle' planes of failure (named torn boudins; Table 1). Drawn boudins are symmetric with no block rotation apparent and no inter-boudin surface (S_{ib}); layer extension was accommodated by differential stretch of both the layer and host. Drawn boudins vary continuously in both the degree of boudin separation and degree of thinning of the interconnecting neck zone. This spectrum is arbitrarily subdivided (Table 1; Fig. 3) into necked boudins with boudin 'blocks' still connected by a neck zone and tapering boudins that are either completely isolated (Fig. 9c), or tenuously connected by particularly long ($M/L \geqslant 0.3$) and thin ($W'W < 0.1$) necks (Fig. 8b).

Necked boudins are also called pinch-and-swell structures in the literature (Ramsay, 1967; Penge, 1976; Lloyd et al., 1982; Van der Molen, 1985). Necked boudin 'blocks' have moderate aspect ratios (L/W averaging 2.6) and are typically of classical boudin shape with bi-convex exteriors and less commonly parallel exteriors with a thinned inter-boudin neck zone ($W'W$ averaging 0.38; Figs. 8b and 9d) associated with host inflow. Vein emplacement accompanied thinning in only 1.4% of investigated cases. Extension of S_e is relatively low with stretch averaging only 129% (Table 2).

Tapering boudin blocks have curved shapes with bi-convex exteriors and terminations that are typically drawn into pointed terminations (Fig. 9c) but can also be rounded, resulting in symmetric boudins with lens/lozenge, or less commonly, sausage shapes (Fig. 9d). Hence the alternative names 'lenticular' boudins (Lloyd et al., 1982) and 'stretched layer' (Lacassin, 1988). Vein infill in the inter-boudin zone is almost entirely absent, with layer extension being accommodated entirely by inflow of the host rock. Aspect ratios (L/W averaging 4.07), extension of the enveloping surface (stretch averaging 177%, with a maximum of 643% in the Kaoko Belt) and isolation of

boudin blocks ($M'L$ averaging 0.69) are all the highest of any boudin type (Table 2). Tapering boudins with high aspect ratios also have high layer extension (M) and boudin isolation (M'), suggesting that at high strain the boudin block is being flattened concomitant with boudin separation.

5.5. Torn boudins

Torn boudins have sharp inter-boudin surfaces (S_{ib}), equivalent to the boudin face, across which there was significant dilation, which is equivalent to layer extension ($M/L = N/L \geq M'L$, which averages 0.41; Figs. 1 and 8c). S_{ib} is at a high angle and typically orthogonal to the boudinaged layer ($\theta \cong \theta'$ averages 85°), resulting in angular, block-shaped boudins also called 'rectangular' or 'extension fracture' boudins (Lloyd and Ferguson, 1981; Lloyd et al., 1982) and 'rectilinear' boudins (DePaor et al., 1991). Torn boudins can be conveniently sub-divided into straight-face and concave-face boudins (Table 1; Fig. 3). The vast majority of boudin block shapes are angular and blocky with parallel exteriors. However, continued stretch of the layer often results in 'burring over' of the boudin edges, concave boudin faces, and bi-convex exteriors, resulting in what has been called 'barrel-shaped' boudins (Lloyd and Ferguson, 1981). The degree of boudin face concave curvature varies continuously (Fig. 3) from straight-face to fishmouth boudins (DePaor et al., 1991; Swanson, 1992; Fig. 9e) which are also called 'fish-head' (Ghosh and Sengupta, 1999) or 'extreme barrel-shaped' boudins (Lloyd and Ferguson, 1981; Lloyd et al., 1982), and ultimately to where the face is folded against itself to resemble false isoclinal folds. Fishmouth boudins are best developed in laminated rock types such as carbonates and by foliation boudinage (Fig. 9e). The boudin face is convex in less than 5% of investigated torn boudins.

Boudin exteriors (Fig. 1) typically remain parallel or slightly convex, but are also rarely concave in the case of bone-type boudins (Malavielle and Lacassin, 1988; Swanson, 1992) that have undergone continued flattening, after vein infill of the inter-boudin zone, resulting in $W'W > 1$ (Fig. 3). The inter-boudin zone of torn boudins is typically filled by vein material (in 74% of investigated cases) containing quartz, K-feldspar, carbonate or micas at greenschist and amphibolite facies and by partial melt at upper-amphibolite to granulite grades. The enveloping foliation is symmetrically drawn into the inter-boudin zone to varying degrees, resulting in scar folds (Hobbs et al., 1976). These are of half wavelength, have peaked (Ramsay, 1967), cuspate or box-fold profiles (Lisle, 1996), which are fold forms generally developed only in association with boudinage.

5.6. Transitions

Typically, only one boudin type is developed within a single boudin train; no mixed trains were recognized. Furthermore, there is minimal overlap or transition between the five end-member boudin block geometries, which on the whole maintain distinct and readily recognizable groups in the field (Figs. 6–8). Transitions between the different groups define a one-dimensional, or linear, spectrum with transitions between drawn and shearband, shearband and domino, domino and sigmoidal-gash, sigmoidal-gash and torn boudins, but apparently not between symmetric boudin types, drawn and torn boudins (Figs. 2, 7 and 8).

There is a transitional continuum between torn and domino boudins. Both θ and θ' in domino boudins vary continuously up to typical torn boudin values of 90° (Fig. 7). Both torn and domino boudins typically develop sharp, planar inter-boudin surfaces; across which dilation is diagnostic of all torn boudins and occurs in 29% of domino boudins as the subset called dilational domino boudins. For most parameters, torn boudins grade progressively into sigmoidal-gash boudins and then domino boudins (Figs. 6–8), thus the latter two can be considered progressively more asymmetric torn boudins. A small proportion of torn boudins (4.5%) show incipient asymmetry with very small displacements and/or block rotations of $<5°$, all of which have domino-type vergences and formed by A-slip boudinage (Table 2). Vergence defined by inclination of S_{ib} shows a weak predominance in torn boudins (56%) to being forward-vergent like in domino-type geometries. At the other end of the domino boudin spectrum, all geometric parameters vary continuously with shearband boudins, such as decreasing α, θ, θ' and N and increasing D (Figs. 6–8). In the field of overlap (i.e. $50° < \theta < 60°$) distinguishing between these two boudin types is unreliable and other qualitative features must be investigated such as the nature of S_{ib}, fringe folds, drag folds and independent shear sense indicators (Goscombe and Passchier, 2003).

There is a transitional continuum in the degree of asymmetry of 'ductile' boudinage types from drawn boudins to shearband boudins (Fig. 2a). Shearband boudins can be considered asymmetric drawn boudins and vice versa. The neck zone in both boudin types is a ductile shear mobile zone, a symmetric coaxial shear zone in drawn boudins and asymmetric non-coaxial shear zone in shearband boudins. At very low angles of θ and θ', the inter-boudin surface of shearband boudins becomes indistinguishable from a highly attenuated neck zone connecting boudin terminations in the case of drawn boudins, and block rotation is barely perceptible (Fig. 7). The angular parameters ('θ' and α) in this transitional field are all $\ll 10°$ and cannot be measured accurately; drawn boudins are characterized by 'θ' $= \alpha = 0°$. The inter-boudin surface in some shearband boudins is not a discrete surface but a wide ductile shear mobile zone displacing adjacent boudins. In these cases, the boudin train has the appearance of asymmetric drawn boudins, which have been described as 'asymmetric pinch-and-swell structures' (Hanmer, 1984, 1986;

Hanmer and Passchier, 1991) and 'type 2A asymmetric pull-apart structures' without discrete S_{ib} (Hanmer, 1986).

6. Boudin train obliquity

The geometry of boudin structures, especially of asymmetric boudins, is not only dependent on material parameters, orientation of S_{ib} during the initial strain increment, bulk flow geometry, metamorphic conditions and strain but also on the initial orientation of the boudinaged element with respect to extension eigenvectors of flow in the rock, also known as fabric attractors, such as contained in the flow plane of simple shear (e.g. Passchier, 1997). The angle between the fabric attractor in the profile plane and the boudin train enveloping surface (S_e) is labelled Ψ in this paper (Figs. 2 and 5a). Boudin trains can be divided into two distinct classes based on boudin train obliquity (Fig. 2c). Boudin trains lying at a low angle to the fabric attractor, for which the final value of Ψ_f attained at the end of deformation is imperceptible in the field and less than a value chosen to be 10°, are classified as foliation-parallel boudin trains (Fig. 2c). All others, where the angle Ψ_f exceeds 10°, are classified as foliation-oblique boudin trains (Fig. 2c). The difference in kinematic behaviour between these two classes is discussed in Goscombe and Passchier (2003).

Boudinage of a material line must necessarily occur in the extensional flow field, but the angle of the boudin train to the fabric attractor is important for their rotational behaviour. Rotation of boudins with respect to the fabric attractors depends on boudin aspect ratio and orientation, whereas the boudin train acts as a material line and rotates towards the attractor in all cases. This can set up relatively complex block rotation of boudins. Boudins can, for example, form in general flow parallel to the flow eigenvector so that individual boudins may rotate forward, but the boudin train is stationary with respect to the fabric attractor, and domino boudins are the result. If the same boudin train is inclined at a high angle (such as 60°) to the attractor, the material line will rotate faster than the boudins, and shearband boudins can form. In general, boudin blocks rotate at a slower rate than the boudin train, and because boudinage will only occur where the boudin train rotates forward into the extensional flow field, foliation-oblique boudin trains typically operate by S-slip boudinage regardless of the shape of the developed boudin block (Fig. 2c; Goscombe and Passchier, 2003). It is therefore important to try to determine the possible orientations of boudin trains with respect to the fabric attractor. Typically the fabric attractor is approximately represented in the rock mass by a penetrative fabric (S_p and L_p), but only if the local deformation history is relatively simple. However, a penetrative foliation may not be developed, or where present, may not represent the fabric attractor associated with boudinage. In practice, it can be difficult to reconstruct the orientation of the fabric attractor, especially if boudins have a complex history, but it is nevertheless important to be aware of the importance of this feature, especially if boudins are to be employed as shear sense indicators or flow regime indicators (Passchier and Druguet, 2002; Goscombe and Passchier, 2003).

Three foliation-oblique boudin train scenarios exist. Unlike foliation-parallel boudin trains, foliation-oblique boudin trains do not necessarily form in association with a penetrative foliation in the rock mass, but are necessarily oblique to the fabric attractor (Fig. 2c). 'Fabric-associated' foliation-oblique boudin trains result where an originally oblique layer (i.e. discordant vein or dyke) is boudinaged during development of the penetrative foliation in the host rock (Fig. 9f). 'Massive' foliation-oblique boudin trains form in discordant layers without development of a penetrative foliation or any other feature approximating the fabric attractor (i.e. vein or dyke in an unfoliated matrix such as in a granite; Hanmer and Passchier, 1991). 'Short-limb' foliation-oblique boudin trains form where the fabric attractor can be inferred to be at an angle to layering and foliation in the rock mass, but with no new fabric developed during boudinage (i.e. boudinage of the over-turned limb during asymmetric folding). In the last two scenarios, a new foliation defining the fabric attractor during boudinage is not necessarily developed. Consequently, these are difficult to recognize as foliation-oblique boudin trains and alternative clues to the obliquity of the fabric attractor must be sought.

Foliation-parallel boudin trains typically form in bedding during development of a bedding-parallel penetrative foliation, and are by far the most numerous type. They comprise 96% of investigated boudin trains in the Kaoko Belt, and this high proportion is probably typical of similar schistose deformation belts that underwent transpressional strain. Four of the five end-member boudin geometry types are developed in both foliation-parallel and foliation-oblique boudin trains, with the exception that gash boudins apparently only form in foliation-parallel boudin trains. The range in, and average values of, geometric parameters in each of the end-member boudin geometries do not differ significantly between foliation-parallel and foliation-oblique boudin trains (Figs. 6–8). Thus the five end-member boudin block geometries remain independent of, and equally distinctive across, the full range of boudin train obliquity. Nevertheless, we have noted that the end-member boudin block geometries are not universally well developed in foliation-oblique boudin trains in all the terranes investigated in this study. This appears to be strongly controlled by the flow regime experienced during boudinage (Goscombe, unpublished data). For example, foliation-oblique domino boudin trains are only recognized in terranes that experienced pure shear flattening, whereas foliation-oblique shearband boudin trains dominate in transpressional terranes that are otherwise devoid of foliation-oblique domino boudin trains.

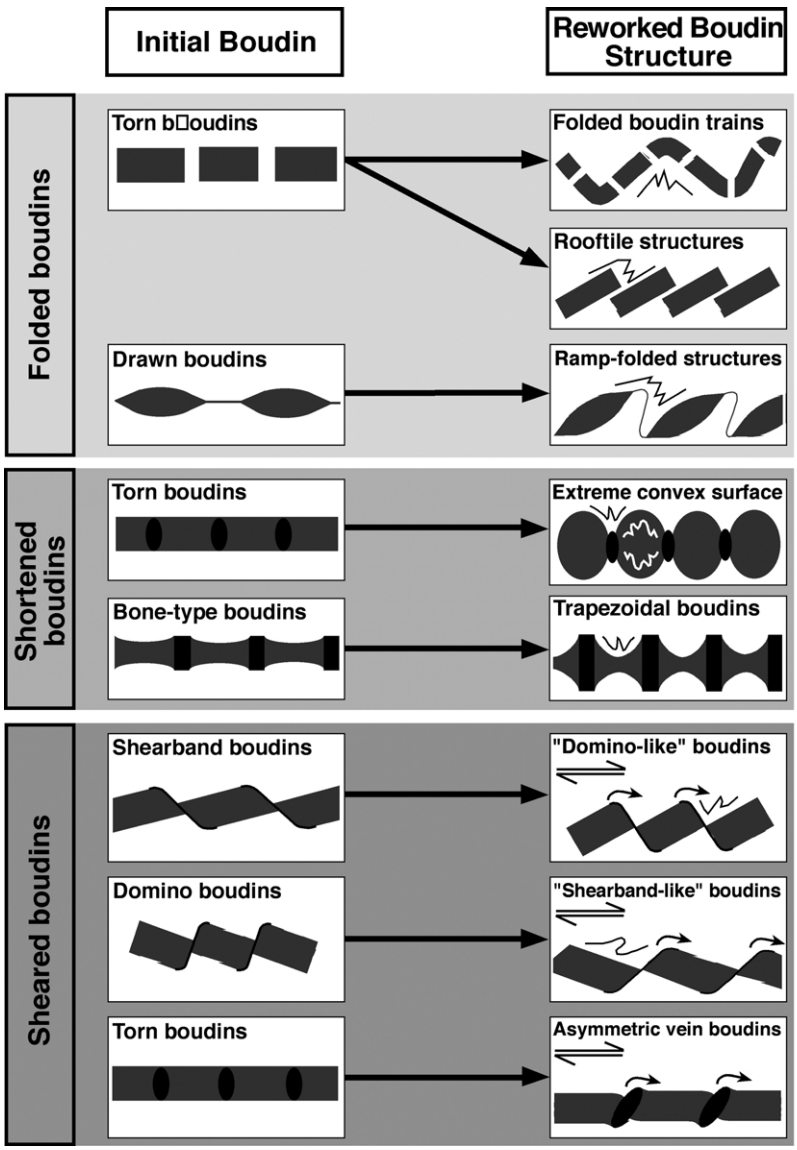

Fig. 10. Classification of reworked boudins that have been modified by a second deformation. Schematic drawings illustrating the most common types recognized in the areas investigated and from the literature. Boudins that have been modified by further stretch (i.e. progressive boudinage) are a special case called sequential boudins that are illustrated in Fig. 11. Symbols as in Fig. 11. Shear sense is dextral in all cases.

7. Modified boudin structures

7.1. Modified boudin structures: theory

A significant subset of investigated boudin structures show evidence for continued deformation of the boudin blocks, after the boudins have separated (Weiss, 1972; Ramsay and Huber, 1983; Hanmer and Passchier, 1991; Carreras and Druguet, 1994). Modified boudins can be classified into two distinct groups (Figs. 10 and 11). (1) Reworked boudin structures experienced shortening subsequent to formation; those shortened in coaxial flow are called shortened boudins, in non-coaxial flow are called sheared boudins and where the boudin train as a whole has been folded, either in coaxial or non-coaxial flow, are called folded boudins (Fig. 10). Reworked boudin structures form where boudins have been subjected to a second phase of deformation separated from the first by a significant period of time, i.e. polyphase, non-congruent structures. (2) Sequential boudin structures experienced continued extension; this can imply that deformation during subsequent episodes was similar to the original condition that caused the boudinage, i.e. progressive congruent structures (Fig. 11). Critical to the interpretation of sequential boudin structures is recognizing successive components of boudinage of different geometric type. Separation of these components is helped by formation of a time marker feature such as vein material, or a change in external conditions such as metamorphic grade, strain or strain rate, between the component events. Non-coaxial or coaxial flow conditions

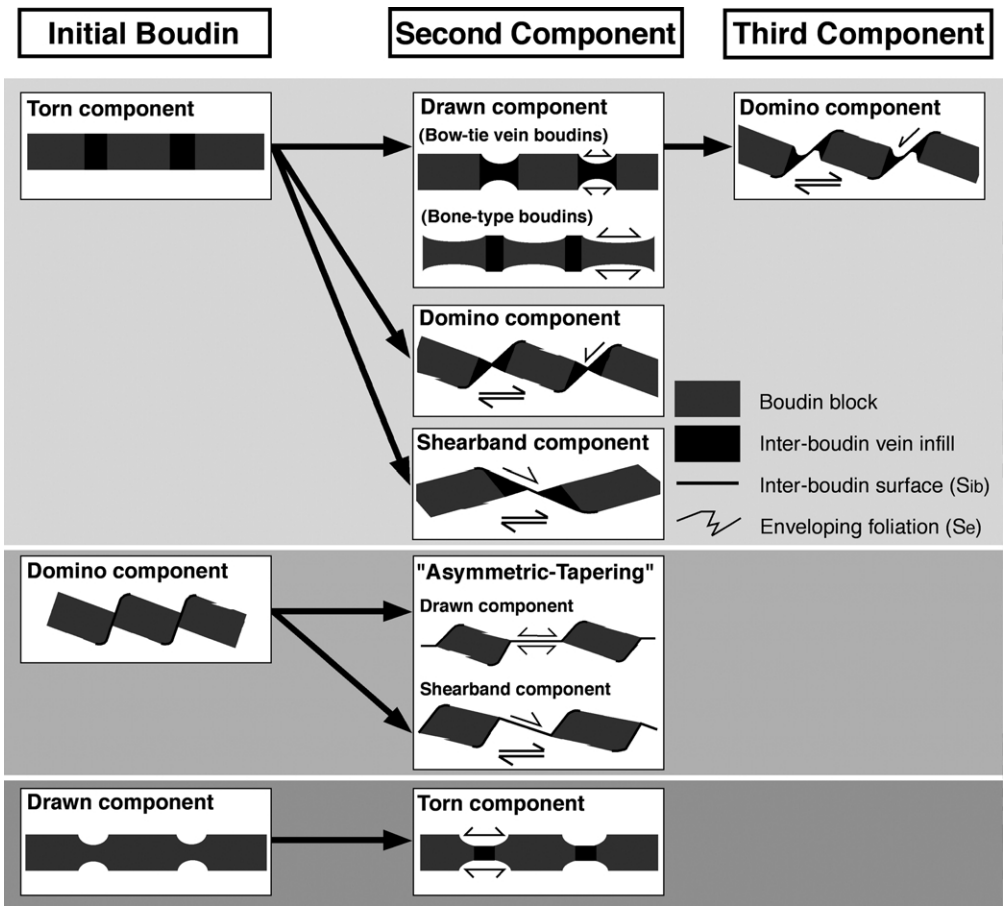

Fig. 11. Schematic drawings of the most common sequential boudins recognized in the areas investigated. Sequential boudin structures are the cumulative result of two or more boudin block geometry components formed during progressive boudinage. Shear sense is dextral in all cases.

do influence further extension of boudins, but mainly in the degree of asymmetry of the structures, which can be weakened or strengthened in this way.

In the discussion of boudin modification it is important to realize that not all combinations of shortening and extension of layers are possible in a flowing continuum. In any type of monoclinic non-coaxial flow with real eigenvectors, i.e. all flow types between simple shear and pure shear, material lines can only rotate from the shortening into the extension field. This means that during continuous deformation, a layer may be first shortened and possibly folded, and then boudinaged, but NOT first boudinaged and then folded. For this reason, if shortened boudins are found, this is evidence for either an unusual flow type without real eigenvectors (rotating flows, like in an eddy), or that deformation is polyphase, with a change in the orientation of principal shortening directions between periods of deformation (Passchier, 1997).

In practice, it may not be possible or useful to determine exactly what combination of deformation was involved in the formation of a modified boudin structure. However, in all cases it is useful to know that such overprints exist, since they indicate a change in the nature of deformation in an area. The main purpose of the following descriptions is to facilitate recognition of modified boudin structures. Some modified boudins are straightforward to recognize, but others may closely resemble simple single-phase boudins. In all cases, crucial information is stored in both the inter-boudin zone and any enveloping foliations present along the boudin exterior. In reworked boudin structures, this includes shortening or folding of inter-boudin vein infill, or solution or crenulation cleavage development in the inter-boudin zone or over the boudin exterior (Fig. 10). Similarly, in sequential boudin structures deformation is typically partitioned into the inter-boudin zone, which is modified into more complex forms (Fig. 11). Note that some folding types can develop as part of the normal boudinage process if part of the fabric is rotated into the shortening field of local flow (i.e. kinkbands associated with shearband boudins). However, such folding will indicate shortening at high angle to the boudin envelope, not parallel to it.

7.2. Reworked boudin structures: overprinting under different external conditions

A significant proportion of the boudins noted in the literature (Weiss, 1972; Ramsay and Huber, 1983; Malavielle and Lacassin, 1988; Hanmer and Passchier, 1991;

Swanson, 1992; Carreras and Druguet, 1994) and in the areas investigated, have been modified to varying degrees by later deformation. In most cases, reworked boudins are easily recognized as structures with disharmonic folding (i.e. shortening) of foliations in the enveloping surface (Fig. 10). Alternatively, boudin blocks may be deformed by a second boudinage event with extension axis at a high angle to the first, such as chocolate tablet boudins. Examples of extensional reworking of boudin structures are rare and hard to distinguish from complex boudin structures that formed in a single event of high flattening strain (Casey et al., 1983; Ghosh, 1988; Aerden, 1991) or in triclinic flow.

7.2.1. Folded boudin structures

Modified boudins are typically, though not always, the result of overprinting subsequent to boudinage by a second, pervasive deformation event. Obvious examples of reworked boudin structures are folded boudin trains (Fig. 10) (Ramberg, 1952; Sengupta, 1983). Where aspect ratios are high, individual boudin blocks may be folded without folding of the boudin train (Sengupta, 1983). If the boudins were wide apart, shortening can stack them like shingles into 'rooftile' structures (Sengupta, 1983; Passchier et al., 1990), and drawn boudins can develop into 'ramp-folded' structures (Fig. 10; Passchier et al., 1990; Price and Cosgrove, 1990). Asymmetric ramp-folded tapering boudins are common in the Kaoko Belt and Damara Orogen in Namibia, and the Himalayan investigation regions. In all of these regions, L_b is parallel to fold axes and the reworked structure apparently formed in one progressive shear event, suggesting a rotating flow scenario (Passchier et al., 1990) where boudin trains rotated from the extensional into the shortening field. Structures with apparent asymmetric ramp-folded forms can also form by attenuation of the overturned limb of a fold without earlier boudinage (Swanson, 1999).

7.2.2. Sheared boudin structures

Boudins may also be reworked by non-coaxial flow, not necessarily with shortening or extension; e.g. when they are parallel to the flow plane of simple shear or another fabric attractor. Layer-parallel shear of symmetric boudins produces asymmetric structures similar to simple asymmetric boudin types, such as torn boudins that are sheared into domino-type or shearband-type geometries. If boudins do not deform much internally, slip on the inter-boudin surface can modify torn boudins into shapes resembling domino boudins. If the boudins do deform internally, shearband boudin shapes can result from either drawn or torn boudins. Torn boudins with inter-boudin vein material result in what we call 'asymmetric vein boudins' that superficially resemble simple dilational domino boudins (Figs. 10 and 12d). These have been called 'asymmetric bone-type boudins' and have been shown to result from layer-parallel shear rotating the inter-boudin veins into a consistently inclined array (Malavielle and Lacassin, 1988; Swanson, 1992). Extreme layer-parallel shear may result in foliation-oblique boudin trains of the earlier formed inter-boudin vein material (Swanson, 1999).

Layer-parallel shear of asymmetric boudin types can change boudin shape by rotation of S_{ib} into either steeper or shallower inclinations and by internal deformation of the boudin blocks (Fig. 10). In high strain, high metamorphic grade ductile terranes, layer-parallel shear can result in the two asymmetric boudin types being oppositely modified and the geometry of the two converging towards each other. For example, layer-parallel shear rotates S_{ib} into lower inclinations (i.e. θ and θ' decrease) in domino boudins, resulting in what we call 'shearband-like' boudins. Conversely, S_{ib} steepens in shearband boudins resulting in 'domino-like' boudins (Fig. 10). Consequently, in high shear-strain, high-grade terranes, domino and shearband boudins may be incorrectly identified and caution must be employed when using these as shear sense indicators (Goscombe and Passchier, 2003). All these examples of sheared boudin structures can potentially look like a simple end-member boudin type and be almost impossible to recognize as reworked boudin structures that experienced polyphase histories. The complex history recorded by the final reworked boudin structure is best indicated by disharmonic folding of the enveloping surface (Fig. 10) and folding of internal layering within boudin blocks (Fig. 12d).

7.2.3. Shortened boudin structures

Shortening by coaxial flow, i.e. symmetric shortening of a layer, results in the most spectacular changes in shape of boudins. If they do not deform much internally, torn boudins can be shortened by compressing the inter-boudin zone, leading to folding of the enveloping foliation that had been drawn into the gap (Fig. 12e). In extreme cases, it can lead to extrusion of foliated matrix material or vein infill out of the inter-boudin zone. In the case of drawn boudins, the thin inter-boudin neck can be folded or affected by pressure solution seams. If folded, the thinnest portion of the neck will show the smallest wavelength of folding as predicted by buckling theory (Ramsay, 1967). If the boudins deform internally, barrel-shaped or blocky boudins may obtain markedly rounded bi-convex exteriors with high B_b ratios, resulting in a curious oval shape with a barrelling effect that is more extreme than anything developed in normal boudins (Fig. 12f). Barrelling such as this is easily recognized where boudin width is significantly greater than the relict undeformed inter-boudin vein material (Fig. 12e and f). Alternatively, shortening of boudins with either parallel or bi-concave exteriors, such as bone-type boudins, will result in 'trapezoidal boudins' if initial boudin block aspect ratios were low (Sengupta, 1983; Fig. 10). Symmetric shortening of asymmetric boudins can lead to reverse faulting reactivation of S_{ib}, and if the boudins are deforming internally, into less asymmetric shapes that may be difficult to recognize as having been reworked. In all cases, foliations and lineations that mantle the boudin train will be shortened and can show the effects of this shortening by

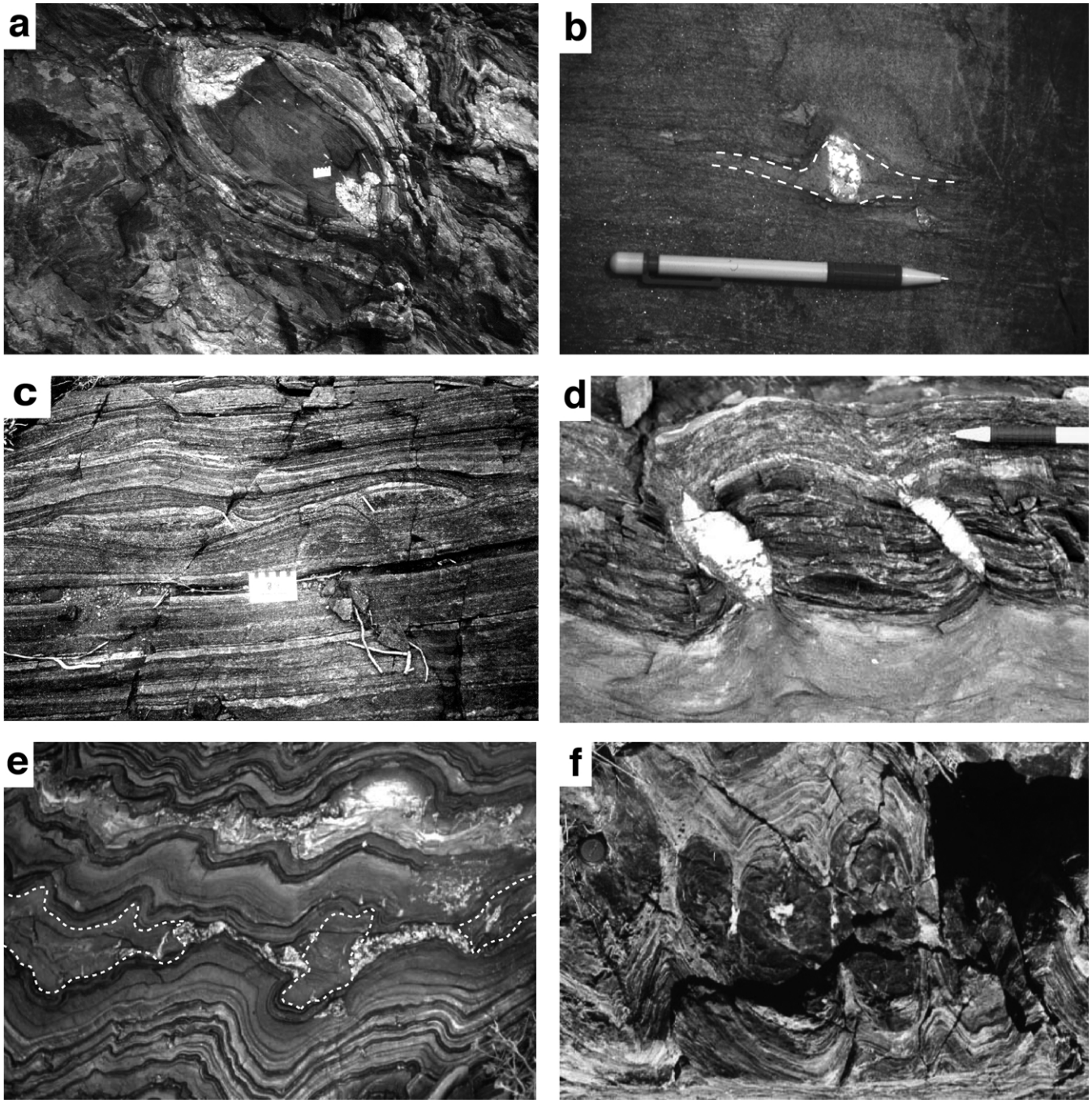

Fig. 12. Examples of modified boudins. Sequential boudin structures ((a)–(c)) are special cases of modified boudins that are formed by progressive stretching resulting in temporally sequential components of different boudin block geometries. (a) Torn boudin with classic barrel boudin geometry of concave face and convex exterior, in mafic gneiss from the Kaoko Belt, Namibia. Progressive boudinage resulted in drawn boudinage of the inter-boudin zone vein infill resulting in an overall tapering boudin geometry. (b) Psammite layer with straight-face torn boudins and quartz-vein infill in the inter-boudin zone, from the Gander Zone in Newfoundland. Progressive boudinage and a change in competence hierarchy resulted in extreme flattening of the original boudin blocks that were drawn without modification of the more competent inter-boudin vein infill. (c) Original domino boudins widely separated by drawn boudinage at higher ductility. Example is in high metamorphic grade quartzo-feldspathic gneisses from the Kaoko Belt in Namibia. Reworked boudin structures (d)–(f). (d) Straight-face torn boudins in a psammite layer from the Ugab Zone, Namibia, have been modified by sinistral foliation-parallel shear. Quartz veins in the inter-boudin zones have been rotated into a consistently inclined array and boudin blocks have been folded in sympathy with the asymmetric tightening of scar folds in the host. (e) Sequential boudin structure from the Ugab Zone, Namibia, that involved progressive boudinage of carbonate layers. Straight-face torn boudins with vein infill were subsequently drawn into tapering boudin geometries. The sequential boudin structures were later modified by shortening along the length of the boudin train, producing thickening and folding of the boudin blocks. (f) Mafic concave-face torn boudins with quartz-vein infill in the inter-boudin zone, from Mount Isa in Australia. The boudin train was later modified by roughly layer-parallel shortening, resulting in thickening of the boudin blocks, producing extreme convex curvature of the exterior. The inter-boudin vein infill provides an approximate indication of the original layer width.

the development of solution seams, crenulation cleavage, small folds or kinks. Crucially, the scar folds in the inter-boudin zone differ in shortened boudin trains by having greatly enhanced amplitudes and tight, pinched hinges (Fig. 12f).

7.3. Sequential boudin structures: overprinting under similar external conditions

Sequential boudin structures are complex boudin structures that evolved through progressive deformation at similar conditions to those in the initial stages of boudinage. That is, they form by continuing stretch of the boudinaged material and document the *ontogenesis*of the structure from initiation to an 'adult' boudin form. Simple end-member boudin block geometries (Fig. 2a) themselves constitute the simplest category of sequential boudin structures, because they are not instantaneously formed. Examples of such gradual modification of boudin shape during one phase of progressive deformation are: (1) the development of domino boudins from a near-orthogonal crack in a layer that develops further by rotation and/or some internal deformation, e.g. that associated with the development of flanking folds (Goscombe and Passchier, 2003); (2) forked-gash and sigmoidal-gash boudins initiate as orthogonal cracks and develop by boudin separation and the inter-boudin vein can either curve (sigmoidal-gash) or branch (forked-gash) at its tips (Goscombe and Passchier, 2003); and (3) concave-face boudins have variably developed 'burring' over the boudin edge resulting in barrel boudins and, with increasing strain, fishmouth boudins and false-isoclinal folds. This is due to the maximum stress being concentrated on the boudin edges, resulting in internal deformation of the boudin block (Lloyd et al., 1982).

More typically, sequential boudin structures record components of different end-member boudin geometries, superimposed in a temporal sequence (Table 2; Fig. 11). Sequential boudins are a special case of modified boudins, involving progressive stretch of the layer, resulting in what can be considered boudinage-modified boudins. Eleven percent of all investigated boudins are sequential boudins. In all examples investigated, there is no evidence for sequential boudins being the result of reworking by subsequent deformational events. All boudin components maintain the same extension axis (L_e) and are consistent with progressive stretch in a single deformation event. Considering the four most common end-member boudin geometry types (drawn, shearband, domino and torn), there are 12 possible permutations of sequential boudins involving two different boudin components. Nine of these have been recorded in our dataset of natural boudin structures; some of these are documented below and their frequency is presented in Appendix B (this can be found in the online version of this paper).

The most common sequence is from a torn boudin component to a drawn boudin component by symmetric extension of a symmetric form (Appendix B). Possibly, this documents either a progression to lower strain rate or prograde metamorphism, and thus more ductile deformation. For example, bow-tie vein (DePaor et al., 1991) and bone-type boudins (Price and Cosgrove, 1990; Swanson, 1992; Fig. 12b) are sequential boudins with an early torn boudin and vein infill component, followed by drawn boudinage of either the inter-boudin vein (Hossein, 1970) or boudin block resulting in these two respective types (Fig. 11). Bone-type boudins develop where the vein material is stronger than the boudin material, resulting in subsequent extension being partitioned into the boudin block, which is stretched. Eight percent of torn boudins in the Kaoko Belt are bow-tie vein boudins (Figs. 3 and 12a); these structures have been noted elsewhere by previous workers (DePaor et al., 1991; Ramsay and Lisle, 2000). In these structures, the $W'W$ ratio of the stretched inter-boudin vein averages 0.54 and is intermediate between torn boudins ($W'W = 1$) and necked boudins ($W'W$ averaging 0.38; Fig. 11).

Evidence of a progression from symmetric to asymmetric boudinage components, such as torn boudins with a later domino boudin component (Swanson, 1992) or shearband boudin component ('intermediate' boudinage of Lacassin (1988); Fig. 11; Appendix B) is also common. In a few sequential boudins, a third component can be recognized, such as domino boudinage of a previously thinned, bow-tie vein boudin (Fig. 11). The opposite, where dilational domino boudins undergo symmetric necking of the inter-boudin vein material, has been modelled in progressive boudinage by Hossein (1970). In the high metamorphic grade areas investigated in the Kaoko Belt, the progression from asymmetric to symmetric boudinage components is common. Domino boudins commonly experienced later extreme ductile stretch—either symmetric (tapering boudinage) or slightly asymmetric (shearband boudinage)—resulting in trains of widely isolated rhomb-shaped boudin blocks (Fig. 11). We have called these 'asymmetric-tapering' boudins. In all investigated cases, the vergence of S_{ib} inclination with respect to bulk shear sense and the high θ angles preserved are consistent with their initial formation as domino boudins (Fig. 12c). Asymmetric-tapering sequential boudins are apparently restricted to high strain, high metamorphic grade ductile terranes.

8. Multiple boudinage events

In all the multiply deformed terranes investigated (Kaoko Belt, Ugab Terrane, Zambezi Belt and Adelaidean Fold Belt), it has been found that boudinage occurred in more than one deformation event. In these terranes, the vast majority of boudins formed early (88% in the Kaoko Belt), during a deformation event that produced a regionally pervasive penetrative fabric, and a minor group of boudins with different orientation formed in a later deformation event. No cases were recorded of

boudinage from two distinct deformation events being superimposed to produce one complex boudin structure. Given the possibility of multiple boudinage events, where boudins are employed as shear sense indicators, flow regime indicators, or indicators of the maximum extension direction (Goscombe and Passchier, 2003), each boudin structure must be correctly correlated with the appropriate deformation event.

Correlation of boudin structure and deformation event is possible because L_e, the theoretical stretching axis associated with boudinage (normal to L_b within S_e; Appendix A), typically has a regular orientation and is both sub-parallel to and symmetrically distributed around the stretching lineation (L_p) produced during the same deformation event (Goscombe and Passchier, 2003). The angle between L_p and L_b (δ;Appendix A) has maximum frequency at 90° (Goscombe and Passchier, 2003). Consequently, L_e is a useful kinematic indicator approximating the axis of maximum finite stretch. Where there are discrete orientation populations of L_b (and by inference also L_e), these could be used to define multiple boudinage events. Where boudins are developed, L_e may be the only kinematic indicator available to define the stretching axis in low-grade, low-strain or fine-grained terranes that are otherwise devoid of stretching lineations. Conversely, in terranes with mineral lineations developed, boudin structures can be employed to test if these mineral lineations are indeed stretching lineations.

9. Conclusions

From this analysis of natural boudin structures, it can be concluded that all simple unmodified boudin structures can be fully classified by considering boudin block geometry, boudin train obliquity and material *layeredness* as summarized graphically in Appendix C (this can be found in the online version of this paper). The entire range of natural boudin block geometries can be rationalized in terms of only five distinctive end-members: drawn, torn, gash, domino and shearband boudins (Fig. 3). The process of boudinage takes place in each case by only one of three mutually exclusive kinematic classes: no-slip, antithetic slip (A-slip) and synthetic slip boudinage (S-slip). Each of these three kinematic classes corresponds almost exclusively to specific boudin block geometries (Table 1). All drawn and torn boudins form by no-slip boudinage, gash and domino boudins by A-slip boudinage and shearband boudins by S-slip boudinage (Goscombe and Passchier, 2003). Transitions between end-member boudin block geometries are recognized in individual geometric parameters (Figs. 2 and 6–8; Table 2). Nevertheless, when the full suite of quantitative geometric parameters and qualitative features are considered, the end-member boudin block geometries remain distinct groupings that are recognizable in the field. We feel that the classification scheme outlined and the following kinematic conclusions are generally applicable as they are based on a comprehensive set of observations and data, from microscopic to macroscopic scales and a wide range of geological settings, flow regimes, rock types and metamorphic grades.

Previous work has resulted in a number of kinematic conclusions with regard to boudins and flow, and these are dependent on the classification scheme outlined here. (1) Given that both the boudin block geometry and an approximation of the fabric attractor can be identified, it has been shown that all boudin geometries in foliation-oblique boudin trains and asymmetric boudins in foliation-parallel boudin trains (Table 2) can be employed as practical and reliable shear sense indicators (Goscombe and Passchier, 2003). (2) It is widely recognized that the near coincidence of the boudin extension axis (L_e) with a mineral stretching lineation (L_p) in many host rocks suggests boudin structures can be used to constrain the stretching axes (transport direction in monoclinic flow) in orogens devoid of mineral stretching lineations, such as in fine-grained, low-strain or low metamorphic-grade terranes (Goscombe and Passchier, 2003).

An important result of the work shown here is that multiple generations of boudins, sequential boudin structures and reworked boudin structures, all record the strain history of a rock mass. Unlike deformation fabrics, boudins are difficult to completely rework and obliterate; thus multiple boudin generations can preserve palaeo-stretching axis directions from different deformational episodes. The suite of boudin types developed during different deformational episodes, and indeed between different study areas, is often distinct. If future workers draw correlations between boudin-type and flow regime, as seems to be the case, boudins may prove useful as indicators of flow regime during different deformational episodes and in characterizing different terranes (e.g. Passchier and Druguet, 2002).

Acknowledgements

Drs Roy Miller, Rudolph Trouw, Fabio Pentagna, Andre Ribeiro, Chris Wilson, Thomas Bekker, Dave Gray and Pat James as well as David and Audrey Goscombe, Helmut Garoeb, Zigi Baugartner, Pete and Alex Siegfried, Murray Haseler and Bonza, are all thanked for their discussions, efforts spying out elusive boudins and great company in the field. The constructive reviews and efforts of Dr L. Goodwin and J. Hippertt were greatly appreciated. This study resulted from regional mapping work undertaken for the Namibian Geological Survey and self-funded fieldwork elsewhere. Mimi Duneski is sincerely thanked for her considerable administrative support and humour in Namibia.

Appendix A. Definition of boudin structural elements and geometric parameters (Fig. 1)

Regional fabric elements

S_p	Penetrative foliation formed in host rock during deformation associated with boudinage.
L_p	Stretching lineation in host rock, for simplicity, considered vector of relative transport during deformation associated with boudinage. Reference frame for linear boudin parameters.
S_e	Enveloping surface of boudinaged layer, equivalent to the overall trace of the boudin train. In most cases parallel to S_p (i.e. foliation-parallel boudin trains) but can be oblique to S_p in the case of foliation-oblique boudin trains. Reference frame for planar boudin parameters
L_e	Extension axis defined by boudin structure. Line normal to the long axis of boudin (L_b), in S_e plane. It is usually close to the X-axis of the finite strain ellipsoid and typically sub-parallel to the stretching lineation (L_p) when developed.
Shear sense	Bulk shear sense during deformation associated with boudinage. Reference frame for all rotational and movement parameters in boudin structures. Defined by C′- and C-type shear band cleavages (Simpson, 1984; Lister and Snoke, 1984), s-type and d-type porphyroclasts (Passchier and Simpson, 1986) and flanking folds (Hudleston, 1989; Passchier, 2001).
Profile plane	Plane normal to both long axis of boudin (L_b) and S_e. Boudins with monoclinic symmetry are viewed and parameters are measured in this plane. In cases of triclinic boudin symmetry, the S_e surface is also used as an additional, orthogonal plane of view.
Fabric attractor	Hypothetical plane or line in rock mass, towards which material lines and planes rotate with progressive deformation (Passchier and Trouw, 1996; Passchier, 1997).

Boudin nomenclature and structural elements

Boudin block	Separate elongate body of rock that originated from boudinage of a layer, object or foliation planes. A string of boudin blocks originating from one layer comprise a boudin train.
Inter-boudin zone	Elongate zone between the edges of adjacent boudin blocks.
Boudin edge	Intersection of a planar boudin face (S_{ib}) and boudin exterior (S_b); parallel to the long axis of both boudin blocks (L_b) and inter-boudin zones.
L_b	Long axis of boudin; equivalent to the "neck line" (Hobbs *et al*. 1976). This line is usually parallel to the intermediate axis (Y) of the finite strain ellipsoid. Equivalent to intersection between S_{ib} and S_b surfaces, that is, the boudin edge (Fig. 1).
L_b vergence	Vergence of acute angle between L_b and stretching lineation (L_p); either clockwise or anticlockwise from the stretching lineation in the S_e surface.
S_b	Boudin exterior; original surface of boudin block in contact with host.
Block rotation	Sense of relative rotation of individual boudin blocks, with respect to bulk shear sense.
Boudin face	Lateral end of boudin block adjacent to others in boudin train, typically a planar or termination face (equivalent to S_{ib}) or a point termination in drawn boudins
S_{ib}	Inter-boudin surface; defined as the median plane in the inter-boudin zone, at moderate to high angle to S_e. In asymmetric boudin structures, is typically a single discrete surface that experienced lateral displacement of adjacent boudins. The S_{ib} surface does not propagate beyond the boudinaged layer (in contrast to faults or shear zones) and in asymmetric boudins, arcs into the enveloping surface at the boudin edge. In torn boudins, S_{ib} is typically equivalent to the terminal face of the boudin block. No S_{ib} is developed in drawn boudins, thus an arbitrary "S_{ib}" is defined as the plane connecting boudin terminations, parallel and median to the extensional mobile zone that is the neck (Fig. 4c).
L_{ib}	Vector of movement within S_{ib}, rarely expressed as slickenlines or mineral elongation lineations.
Slip sense	Sense of lateral displacement along S_{ib}, with respect to bulk shear sense.
S_{ib} vergence	There are two types of vergence of S_{ib} with respect to bulk shear sense: (1) Spiral vergence, analogous to sygmoidal tension gashes, and (2) Direction of inclination of S_{ib} with respect to bulk shear sense; those inclined in opposite direction to shear sense are named forward-vergent and those inclined in

the same direction as shear sense are named backward-vergent. These are equivalent to "forward-tilted" and "backward-tilted" respectively (Swanson 1992), which are defined by an imagined tilting of S_{ib} from an originally orthogonal orientation, with respect to bulk shear sense. In the case of gash boudins, both types of vergence are observed on both the profile and S_e planes of view.

"Drag" on S_{ib} — Sense of apparent drag on boudin face, with respect to slip sense. Can be either antithetic (flanking folds) or synthetic (flanking shear band; Fig. 5; Passchier, 2001). Flanking folds on S_{ib} contribute an additional component of block rotation that is synthetic with whole block rotation. Flanking folds on S_{ib} are not to be confused with the flanking folds that formed by similar mechanism, but of different scale and site, on the margin of the trace of foliation-oblique boudin trains (Fig. 5).

Angular parameters

δ — Acute angle between L_p and L_b, an approximate measure of the degree of departure from monoclinic symmetry. A boudin structure of monoclinic symmetry has d = 90°.

α — Relative block rotation; is the acute angle between S_e and S_b.

θ — Acute angle between S_b and S_{ib}; quantifying boudin block shape.

θ' — Acute angle between S_{ib} and S_e; quantifying S_{ib} inclination in outcrop: $\theta' = \theta - \alpha$.

β — Angle between S_{ib} and axial surface of associated kinkbands. Measured from S_{ib} synthetic with respect to slip sense on S_{ib}, and so may be acute or obtuse.

Ψ — Obliquity of boudin train; measured as the angle between S_e and the fabric attractor, which is assumed in most cases to approximate the penetrative foliation (S_p).

Dimensional parameters

W — Width or thickness of boudinaged layer.

W′ — Minimum width of thinned layer or vein infill in the inter-boudin zone.

L — Length of boudin blocks in the profile plane.

Q — Extent of the boudin block parallel to L_b. Typically greater than the extent of the outcrop and thus effectively infinite.

M — Component of extension of boudinaged layer, parallel to S_e and normal to L_b. Measured between boudin edges in asymmetric and torn boudins and between inflection points (Penge, 1976) in the termination or neck zone of drawn boudins (Fig. 1d).

M′ — Degree of isolation of adjacent boudin blocks, parallel to S_e and normal to L_b. Equivalent to "gap length" (Lloyd *et al.*, 1982). $M' < M$ in asymmetric boudins and $M' = M$ is only possible in symmetric boudins.

N — Amount of dilation normal to, and across, S_{ib}. Not applicable to drawn boudins with arbitrary "S_{ib}", minor for asymmetric boudins and significant in torn boudins where with $N \cong M \cong M'$.

D — Lateral displacement along S_{ib} between adjacent boudin blocks.

Stretch — Percent extension of the enveloping surface (S_e): Stretch $= 100(M + L\cos\alpha)/L$. Considers the extension of a line (S_e), not a layer of finite width, thus stretch can only be considered minimum value of layer extension and stretch $<100\%$ can occur for low M and high a boudins.

B_b — Ratio describing the curve of the boudin exterior (Fig. 4). Defined by the height above (+ve) or below (−ve) the line between boudin edges, divided by length of the straight line between edges (i.e. L).

B_f — Ratio describing the curve of the boudin face (Fig. 4). Defined by the distance out (+ve) or into the boudin block (−ve) from the line between boudin edges, divided by the straight line length of this face line.

References

Aerden, D.G.A.M., 1991. Foliation-boudinage control on the formation of the Rosebery Pb–Zn orebody, Tasmania. Journal of Structural Geology 13, 759–775.

Blumenfeld, P., 1983. Le "tuilage des megacristaux", un critère d'écoulement rotationnel pour les fluidalites des roches magmatiques; Application au granite de Barbey. Bulletin de la Société géologique de France 25, 309–318.

Borradaile, G.J., Bayly, M.B., Powell, C.McA., 1982. Atlas of Deformational and Metamorphic Rocks Fabrics, Springer-Verlag, Berlin, Heidelberg, New York, 649pp.

Bosworth, W., 1984. The relative roles of boudinage and 'structural slicing' in the disruption of layered rock sequences. Journal of Geology 92, 447–456.

Carreras, J., Druguet, E., 1994. Structural zonation as a result of

inhomogeneous non-coaxial deformation and its control on syntectonic intrusions: an example from the Cap de Creus area, eastern-Pyrenees. Journal of Structural Geology 16, 1525–1534.

Casey, M., Dietrich, D., Ramsay, J.G., 1983. Methods for determining deformation history for chocolate tablet boudinage with fibrous crystals. Tectonophysics 92, 211–239.

Conti, P., Funedda, A., 1998. Mylonite development in the Hercynian basement of Sardinia (Italy). Journal of Structural Geology 20, 121–133.

Daniel, J.-M., Jolivet, L., Goffe, B., Poinssot, C., 1996. Crustal-scale strain partitioning: footwall deformation below the Alpine Oligo–Miocene detachment of Corsica. Journal of Structural Geology 18, 41–59.

Davis, G.H., 1987. A shear-zone model for the structural evolution of metamorphic core complexes in southeastern Arizona. Continental Extensional Tectonics, Geological Society Special Publication 28, 247–266.

DePaor, D.G., Simpson, C., Bailey, C.M., McCaffrey, K.J.W., Bean, E., Gower, R.J.W., Aziz, G., 1991. The role of solution in the formation of boudinage and transverse veins in carbonate rocks at Rheems, Pennsylvania. Geological Society of America Bulletin 103, 1552–1563.

Etchecopar, A., 1974. Simulation par ordinateur de la deformation progressive d'un aggregat polycrystallin. Étude du développement de structures orientées par écrasement et cisaillement. Unpublished Ph.D. thesis, University of Nantes, France.

Etchecopar, A., 1977. A plane kinematic model of progressive deformation in a polycrystalline aggregate. Tectonophysics 39, 121–139.

Fry, N., 1984. The Field Description of Metamorphic Rocks, Geological Society of London Handbook Series, Open University Press, Milton Keynes, 110pp.

Ghosh, S.K., 1988. Theory of chocolate tablet boudinage. Journal of Structural Geology 10, 541–553.

Ghosh, S.K., Sengupta, S., 1999. Boudinage and composite boudinage in superimposed deformations and syntectonic migmatization. Journal of Structural Geology 21, 97–110.

Goldstein, A.G., 1988. Factors affecting the kinematic interpretation of asymmetric boudinage in shear zones. Journal of Structural Geology 10, 707–715.

Goscombe, B., 1991. Intense non-coaxial shear and the development of mega-scale sheath folds in the Arunta Block, Central Australia. Journal of Structural Geology 13, 299–318.

Goscombe, B., 1992. High-grade reworking of central Australian granulites. Part 1. Structural evolution. Tectonophysics 204, 361–399.

Goscombe, B., Everard, J.L., 2000. Tectonic evolution of Macquarie Island: extensional structures and block rotations in oceanic crust. Journal of Structural Geology 23, 639–673.

Goscombe, B., Passchier, C.W., 2003. Asymmetric boudins as shear sense indicators—an assessment from field data. Journal of Structural Geology 25, 575–589.

Grasemann, B., Stuwe, K., 2001. The development of flanking folds during simple shear and their use as kinematic indicators. Journal of Structural Geology 23, 715–724.

Hanmer, S.K., 1984. The potential use of planar and elliptical structures as indicators of strain regime and kinemetics of tectonic flow. Current Research, Part B, Geological Survey of Canada, Paper 84-1B, pp. 133–142.

Hanmer, S., 1986. Asymmetrical pull-aparts and foliation fish as kinematic indicators. Journal of Structural Geology 8, 111–122.

Hanmer, S., 1989. Initiation of cataclastic flow in a mylonite zone. Journal of Structural Geology 11, 751–762.

Hanmer, S., Passchier, C., 1991. Shear-Sense Indicators: A Review. Geological Survey of Canada. Paper 90-17, 72pp.

Hobbs, B.E., Means, W.D., Williams, P.F., 1976. An Outline of Structural Geology. John Wiley and Sons, 278–280.

Hossein, K.M., 1970. Experimental work on boudinage. Unpublished M.Sc. thesis, Imperial College, University of London.

Hudleston, P.J., 1989. The association of folds and veins in shear zones. Journal of Structural Geology 11, 949–957.

Jones, A.G., 1959. Vernon map-area British Columbia. Memoir Geological Survey Branch, Canada 296, 1–186.

Kraus, J., Williams, P.F., 1998. Relationships between foliation development, porphyroblast growth and large-scale folding in the metaturbidite suite, Snow Lake, Canada. Journal of Structural Geology 20, 61–76.

Lacassin, R., 1988. Large-scale foliation boudinage in gneisses. Journal of Structural Geology 10, 643–647.

Laubach, S.E., Reynolds, S.J., Spencer, J.E., 1989. Progressive deformation and superposed fabrics related to Cretaceous crustal underthrusting in western Arizona, USA. Journal of Structural Geology 11, 735–749.

Lisle, R., 1996. Cover photograph. Journal of Structural Geology 18.

Lister, G.S., Snoke, A.W., 1984. S–C mylonites. Journal of Structural Geology 6, 617–638.

Lloyd, G.E., Ferguson, C.C., 1981. Boudinage structure: some new interpretations based on elastic–plastic finite element simulations. Journal of Structural Geology 3, 117–128.

Lloyd, G.E., Ferguson, C.C., Reading, K., 1982. A stress-transfer model for the development of extension fracture boudinage. Journal of Structural Geology 4, 355–372.

Lohest, M., 1909. L'origine des veines et des géodes des terrains primaires de Belgique. Annales de la Société géologique Belgique 36B, 275–282.

Malavielle, J., Lacassin, R., 1988. 'Bone-shaped' boudins in progressive shearing. Journal of Structural Geology 10, 335–345.

Mandal, N., Karmakar, S., 1989. Boudinage in homogeneous foliation rocks. Tectonophysics 170, 151–158.

Mullenax, A.C., Gray, D.R., 1984. Interaction of bed-parallel stylolites and extension veins in boudinage. Journal of Structural Geology 6, 63–71.

Passchier, C.W., 1997. The fabric attractor. Journal of Structural Geology 19, 113–127.

Passchier, C.W., 2001. Flanking structures. Journal of Structural Geology 23, 951–962.

Passchier, C.W., Druguet, E., 2002. Numerical modelling of asymmetric boudinage. Journal of Structural Geology 24, 1789–1804.

Passchier, C.W., Simpson, C., 1986. Porphyroclast systems as kinematic indicators. Journal of Structural Geology 8, 831–843.

Passchier, C.W., Myers, J.S., Kröner, A., 1990. Field Geology of High-Grade Gneiss Terrains, Springer-Verlag, Berlin, 150pp.

Penge, J., 1976. Experimental deformation of pinch-and-swell structures. Unpublished M.Sc. thesis, Imperial College, University of London.

Price, N.J., Cosgrove, J.W., 1990. Analysis of Geological Structures, Cambridge University Press, Cambridge.

Ramberg, H., 1952. The Origin of Metamorphic and Metasomatic Rocks, University of Chicago Press, Chicago.

Ramsay, A.C., 1881. The Geology of North Wales. Memoirs of the Geological Survey of Great Britain, 3.

Ramsay, J.G., 1967. Folding and Fracturing of Rocks, McGraw-Hill, New York, pp. 103–109.

Ramsay, J.G., Huber, M.I., 1983. The Techniques of Modern Structural Geology. Volume 1: Strain Analysis, Academic Press, London, pp. 1–224.

Ramsay, J.G., Huber, M.I., 1987. The Techniques of Modern Structural Geology. Volume 2: Folds and Fractures, Academic Press, London, pp. 516–633.

Ramsay, J.G., Lisle, R., 2000. The Techniques of Modern Structural Geology. Volume 3: Application of Continuum Mechanics in Structural Geology, Academic Press, London.

Roig, J.-Y., Faure, M., Truffert, C., 1998. Folding and granite emplacement inferred from structural, strain, TEM and gravimetric analyses: the case study of the Tulle antiform, SW French Massif Central. Journal of Structural Geology 20, 1169–1189.

Sengupta, S., 1983. Folding of boudinaged layers. Journal of Structural Geology 5, 197–210.

Simpson, C., 1984. Borrego Springs–Santa Rosa mylonite zone: a Late Cretaceous west-directed thrust in southern California. Geology 12, 8–11.

Simpson, C., Schmid, S.M., 1983. An evaluation of criteria to deduce the

sense of movement in sheared rocks. Bulletin of the Geological Society of America 94, 1281–1288.

Swanson, M.T., 1992. Late Acadian–Alleghenian transpressional deformation: evidence from asymmetric boudinage in the Casco Bay area, coastal Maine. Journal of Structural Geology 14, 323–341.

Swanson, M.T., 1999. Kinematic indicators for regional dextral shear along the Norumbega fault system in the Casco Bay area, coastal Maine. Geological Society of America Special Paper 331, 1–23.

Van der Molen, I., 1985. Interlayer material transport during layer-normal shortening. Part II. Boudinage, Pinch-and-swell and migmatite at Sondre Stromfjord Airport, West Greenland. Tectonophysics 115, 297–313.

Weiss, L.E., 1972. The Minor Structures of Deformed Rocks, Springer-Verlag, Berlin, 431pp.

Wilson, G., 1961. The tectonic significance of small-scale structures and their importance to the geologist in the field. Annals of the Society of Geologists de Belgique 84, 424–548.

Yamamoto, H., 1994. Kinematics of mylonitic rocks along the Median Tectonic Line, Akaishi Range, central Japan. Journal of Structural Geology 16, 61–70.